# ADAPTIVE OBSERVER AND SLIDING MODE OBSERVER BASED ACTUATOR FAULT DIAGNOSIS FOR CIVIL AIRCRAFT

by

Guangqing Jia

B.A.Sc., Beijing Institute of Technology, Beijing, China, 1997

A THESIS SUBMITTED IN PARTIAL FULFILLMENT
OF THE REQUIREMENTS FOR THE DEGREE OF
MASTER OF APPLIED SCIENCE
in the School
of
Engineering Science

© Guangqing Jia 2006

SIMON FRASER UNIVERSITY


Summer 2006

All rights reserved. This work may not be
reproduced in whole or in part, by photocopy
or other means, without the permission of the author.

# APPROVAL

**Name:** Guangqing Jia

**Degree:** Master of Applied Science

**Title of Thesis:** Adaptive Observer And Sliding Mode Observer Based Actuator Fault Diagnosis For Civil Aircraft

**Examining Committee:** Dr. John Bird, Chair
Professor, School of Engineering Science
Simon Fraser University

---

Dr. Mehrdad Saif, Senior Supervisor
Professor, School of Engineering Science
Simon Fraser University

---

Dr. Shahram Payandeh, Supervisor
Professor, School of Engineering Science
Simon Fraser University

---

Dr. William A. Gruver, Examiner
Professor, School of Engineering Science
Simon Fraser University

**Date Approved:** July 31, 2006


SIMON FRASER UNIVERSITY library

# DECLARATION OF PARTIAL COPYRIGHT LICENCE

The author, whose copyright is declared on the title page of this work, has granted to Simon Fraser University the right to lend this thesis, project or extended essay to users of the Simon Fraser University Library, and to make partial or single copies only for such users or in response to a request from the library of any other university, or other educational institution, on its own behalf or for one of its users.

The author has further granted permission to Simon Fraser University to keep or make a digital copy for use in its circulating collection, and, without changing the content, to translate the thesis/project or extended essays, if technically possible, to any medium or format for the purpose of preservation of the digital work.

The author has further agreed that permission for multiple copying of this work for scholarly purposes may be granted by either the author or the Dean of Graduate Studies.

It is understood that copying or publication of this work for financial gain shall not be allowed without the author's written permission.

Permission for public performance, or limited permission for private scholarly use, of any multimedia materials forming part of this work, may have been granted by the author. This information may be found on the separately catalogued multimedia material and in the signed Partial Copyright Licence.

The original Partial Copyright Licence attesting to these terms, and signed by this author, may be found in the original bound copy of this work, retained in the Simon Fraser University Archive.

Simon Fraser University Library
Burnaby, BC, Canada

# Abstract

Aircraft modelling based on Research Civil Aircraft Model (RCAM) is first introduced in this work. The actuator fault isolation problem for the aircraft is then investigated. An adaptive observers (AO) and a sliding mode observers (SMO), were chosen for fault diagnosis purposes. An adaptive scheme based on a bank of AOs is designed to detect and isolate constant actuator faults. Theoretical results are obtained to ensure that the proposed schemes can work well for actuator fault diagnosis under certain assumptions. Simulation results on RCAM show that the adaptive observer based technique can detect and isolate constant actuator faults successfully. However, the adaptive scheme can not deal with non-constant actuator faults (which may also occur in civil aircrafts). It also can not estimate the actuator faults which may be crucial for fault accommodation purpose.As an addictive, in order to deal with non-constant actuator faults and to estimate the faults, an SMO based scheme is proposed for fault detection, isolation and estimation. This method can be used for any types of faults. Under certain assumptions, it is proved the SMO based scheme can detect, isolate, and estimate various actuator faults. A number of simulations studies are performed on RCAM model for various abrupt and incipient actuator faults. The results show that both abrupt and incipient faults can be detected and isolated successfully, which is consistent with the analysis. Moreover, both abrupt and incipient faults can be estimated very accurately. Although fault accommodation is not addressed in this work, it is important to note that accurate estimation of faults can lead to a more solid fault diagnosis decisions and can provide useful information for fault accommodation purpose.

# Acknowledgements

I would like to thank the following people for contributing so much to the completion of this thesis. With the leadership, example, and support of each of the individuals below, I have managed to learn, enjoy, and grow through what will surely be some of the best years of my life.

I wish first to express my sincere gratitude to my supervisor Dr. Mehrdad Saif, for his guidance, encouragement and support that he have given me. I would like to thank Dr. Shahram Payandeh, for his kindly supervision. Special thanks to Dr. William Gruver, for teaching me system and control theory. Many thanks for giving me the opportunity to be his assistant, upon which I built much of my knowledge and lecture experiences. I give thanks to Dr. William Gruver for his advice of the style and writing of my thesis. Special thanks to Dr. John Bird for chairing my thesis defence.

Thank you Dr. Weitian Chen, Dr. Wen Chen and Mr. Qing Wu for giving me the opportunity to work with you. Thank you also to the staffs in the department. Thank you for helping make confusing paperwork more understandable, and for helping make my experience at SFU wonderful. Also, thank you so much to my past and present labmates, Amir Masoud Niroumand, Jimmy Tsai, Guoyu Wang, Jennifer Liu, for always being there with help and encouragement.

Finally, I am grateful to my family. To my wife Xu Han for your unconditional love and support that you have given me. I could not have done it alone. To my mom and dad, brother and in-laws, for your supports, patience, and sacrifices.

# Dedication

I dedicate this thesis to my wife Xu Han, and my parents.

# Table of Contents

# List of Figures

# List of Tables

# Nomenclature

| | |
|---|---|
| $e_{x_i}$ | error between $\hat{x}_i$ and $x$. |
| $p$ | roll rate(in $F_B$) |
| $q$ | pitch rate(in $F_B$) |
| $r_i(t)$ | $i$th residual. Defined as $r_i(t) = \|\|e_{x_i}(t)\|\|^2$. |
| $r$ | yaw rate(in $F_B$) |
| $u_j^f$ | faulty output of $j$th actuator. |
| $u_B$ | x component of inertial velocity in $F_B$ |
| $V_A$ | airspeed |
| $v_B$ | y component of inertial velocity in $F_B$ |
| $w_B$ | z component of inertial velocity in $F_B$ |
| $w_V$ | $z$ component of inertial velocity in $F_V$ |
| X $x$ | state vector. |
| $X$ | x position of aircraft CoG in $F_E$ |
| $\hat{x}_i$ | estimated $x$ from the $i$th oberver. |
| $Y$ | y position of aircraft CoG in $F_E$ |
| $Z$ | z position of aircraft CoG in $F_E$ |
| $\alpha$ | angle of attack(AOA) |
| $\delta_T$ | tailplane deflection. |
| $\delta_{TH}$ | throttle position of engine. |
| $\phi$ | roll angle(Euler angle) |
| $\theta$ | pitch angle(Euler angle) |
| $\psi$ | heading angle(Euler angle) |

# Table of Acronyms

| | |
|---|---|
| CoG | Center of Gravity |
| FAA | Federal Aviation Authority |
| FDI | Fault Detection and Isolation |
| ICAO | International Civil Aviation Organization |
| NASA | National Aeronautics and Space Administration |
| NED | North-East-Down Axis system |
| RCAM | Research Civil Aircraft Model |
| SMO | Sliding Mode Observer |

# Chapter 1

# Introduction

Fatal airplane crashes cause tragic loss of life and are accompanied by colossal expenses associated with destruction of property, cost of investigation, and reduced public confidence. Over the last three decades, the growing demand for reliability, maintainability, and survivability in technical systems has drawn significant research in Fault Detection and Isolation(FDI). Faults can occur in both hardware and software used in an airplane systems. This thesis focuses on hardware faults. A *fault* that tends to degrade the overall system performance, represents an undesired change, whereas a *failure* denotes a complete breakdown of a component or function. In this thesis, fault rather than failure is used to indicate a tolerable malfunction, rather than a catastrophe.

Several regularities and investigative agencies are advocating the use of technologies that will further reduce fatal accidents. Which are presently less than one per million departures, not including sabotage, terrorism and military action, making air travel the safest mode of transport. 2004 was the safest in aviation history compared with 2003 [2], and aviation remains the safest form of transport. Fatalities were down to 428, a reduction of more than 35 % compared with 2003, and the accident rate

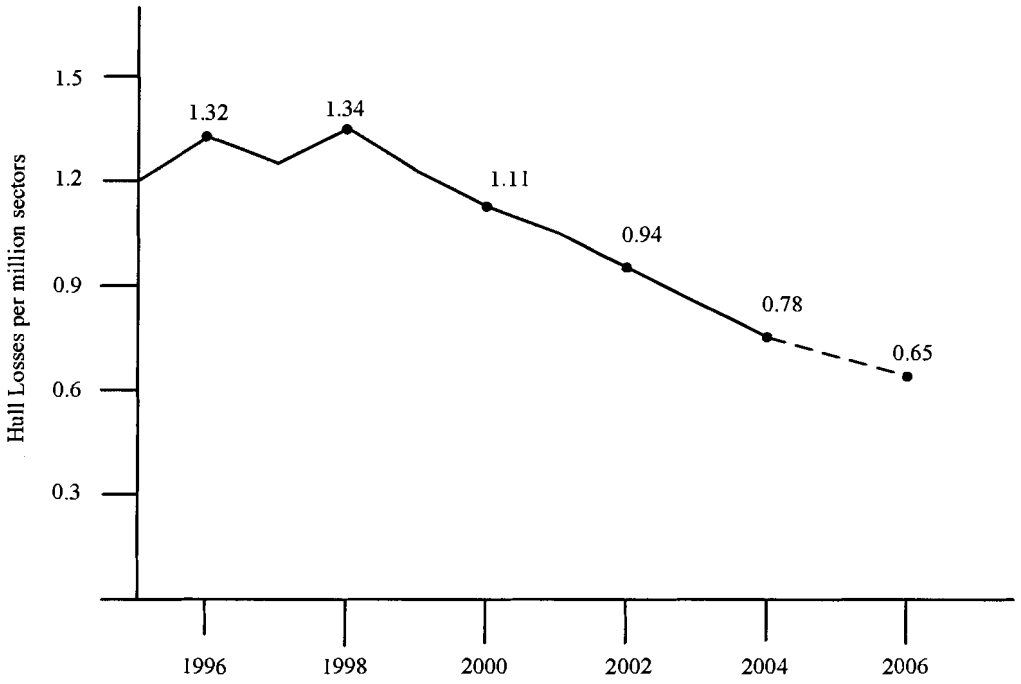


Figure 1.1: Hull Losses per Million Sectors

dropped 10 %, to 0.78 for western-built jet hull losses[1] per million sectors. But there is still work to be done [3]. In 2004, the industry set a target for 25 % reduction in the accident rate by year-end 2006 (Figure 1.1). In many cases, human errors and deficient airport facilities are cited as causes by the investigative agencies for these accidents [3]. Present challenges are not easily overcome. However, numerous aircraft accidents in the recent years have been caused when components in the control loop malfunctioned. Failed sensors or actuators, such as faulty gyros, stuck horizontal stabilizers or other control surfaces failures have led to catastrophic consequences.

Lock-in-place and hard-over faults of safety-critical effectors present an important practical problem. In the Lock-in-place case, the effector locks (" freezes ") in a fixed

[1]National Transportation Safety Board (NTSB) and International Civil Aviation Organization (ICAO) definition of Hull loss: Airplane damage that is substantial and is beyond economic repair. Hull loss also includes events in which: airplane is missing or search for wreckage has been terminated without it being located or the airplane is substantially damaged and inaccessible.

position, which can occur, for example, due to a jammed electro-mechanical actuator. In the hard-over case, the control surfaces actuated by an electro-hydraulic actuator, locks in its extreme position due to a failure of hydraulic system components. In general, feedback control algorithms designed to handle small system perturbations that arise under normal operating conditions, are not useful [4]. There is need to design fault detection and identification schemes which actively address failures in the control loop. Automated maintenance for early detection of malfunctioned equipment is a crucial problem in many applications. To satisfy the needs for safety, reliability, and performance in the aviation industry, it is important to detect system component faults, actuator faults, and sensor faults, and to accurately diagnose the source and severity of each malfunction so that corrective actions can be taken.

The nominal controller performs inadequately because of the changes in the system dynamics following a failure. Fault accommodation schemes need to be considered after a failure in the aircraft system. A possible approach for fault accommodation is to predesign various observers, anticipating component failures and then accommodating the fault when the component failure is detected. The key to design a bank of observers is to expedite the redundancy in the aircraft sensing and actuation. Modern aircraft are instrumented with redundant sensors and have many control surfaces that may be used even with some failures. Once these observers are designed, they can be implemented in the on-board computer. A supervisory accommodation scheme can be designed based on the failure detection and identification mechanism.

In this thesis, the design of observers for detecting and accommodating actuator faults is considered. The ability to design observers for actuator failure is linked to the property of the system, which allows the design of stable observers for the purpose of reconstructing the states for using state feedback. However, actuator failures are not

only related to the stabilizability or controllability of the system. When actuators fail they not only reduce control authority, but also may present persistent disturbances. For which the functional actuators must compensate. It is shown that the problem of predesigning a controller for lock-in-place and hard-over actuators can be reduced to design a regulator with internal stability.

The utility of observer design techniques is illustrated using flight control examples. In the next section, the organization of the thesis is described.

## 1.1 Motivation

In 1959, which was the first full year of commercial jet operations, the world's air carriers averaged 100,000 jet-flying hour per hull loss. In 1999, they average nearly 800,000 flying hours per hull loss [5]. The record varies globally; even so, air transportation is the safest of all major modes of transportation. However, the current accident rate, which is under one per million departures, will be soon become unacceptable because of the predicted increase in the commercial air traffic, that is expected to triple from 1998 to 2018 [6]. Several agencies including the regulatory authority Federal Aviation Authority (FAA), National Aeronautics and Space Administration (NASA), International Civil Aviation Organization (ICAO), and nonprofit organizations like the Flight Safety Foundation and Aviation Safety Network are advocating for a significant reduction in airplane accidents [7, 8]. For example, in November 1999, NASA Langley Research Center announced to "Reduce the aircraft accident rate by a factor of 5 within 10 years, and by a factor of 10 within 25 years" [9].

A modern aircraft has a few million parts, e.g. a Boeing 767 has approximately 3,140,000 parts. Although, each of these parts are tested, the likelihood of a part malfunction is large. Many accidents can be directly linked to the failures of control

system components.

Months of investigation by authorities are needed to determine the exact sequence of events that lead to a fatal air crash. Sometimes these investigations are inconclusive and it is left to the imagination as to what may have gone wrong with the airplane. Some recent examples of fatal accidents that may have been caused by failures in the control loop components are as follows [10].

1. The Alaska Airline Flight 261, January 2000: On January 31, McDonnell Douglas MD-83 crashed off the coast of California about 4:20 p.m. (PST) en route from Puerto Vallarta, Mexico, to San Francisco, killing all of its 83 passengers and 5 members of the crew.

   The investigation shows clearly from the flight data recorder that the crew was unable to maintain vertical control due to a dysfunctional stabilizer. The Flight Data Recorder shows that the stabilizer trim changed to a full-nose down trim and remained jammed there until the crash. During the last 12 minutes before the crash the crew attempted to diagnose and troubleshoot their stabilizer trim problems in vain and the MD-83 finished just off Point Mugu, CA, 650 ft deep in water. The failure of the actuation assembly during the final minutes of flight was confirmed when the navy recovered the parts from the sea. It can be hypothesized that mechanical failure of the actuation assembly of the horizontal stabilizer was the primary cause of the tragic accident.

2. Air Midwest Flight 5481 of January 2003: On January 8, about 08:47:28 Eastern Standard Time, a Raytheon (Beechcraft) 1900D crashed shortly after takeoff from runway 18R at Charlotte-Douglas Airport, Charlotte, North Carolina. Two flight crew members and nineteen passengers were killed, one person on

the ground received minor injuries, and the aircraft was destroyed by impact forces and a post crash fire.

The National Transportation Safety Board determined that the probable cause of this accident was loss of pitch control during takeoff, resulting from the incorrect rigging of the elevator control system compounded by the aft center of gravity, which was substantially moving backward of the certified limit.

3. American Airlines Flight 587 of November 2001: On November 12, 2001, about 09:16:15 Eastern Standard Time, an Airbus Industrie A300-605R crashed into a residential area of Belle Harbor, New York, shortly after takeoff from John F. Kennedy International Airport. Flight 587 was a regularly scheduled passenger flight to Las Americas International Airport, Santo Domingo, Dominican Republic. All 260 passengers and five people on the ground were killed, and the aircraft was destroyed by impact forces and a post crash fire.

   The National Transportation Safety Board determined that the probable cause of this accident was in-flight separation of the vertical stabilizer as a result of loads beyond acceptable limits that were created by unnecessary and excessive rudder pedal inputs by the pilots. Contributing to these rudder pedal inputs were characteristics of the Airbus A300-600 rudder system and elements of the American Airlines Advanced Aircraft Maneuvering Program. The safety issues focued on characteristics of the A300-600 rudder control system design, A300-600 rudder pedal inputs at high airspeeds, aircraft-pilot coupling, flight operations at or below design maneuvering speed, and upset recovery training programs.

This list is not exhaustive but only representative of fatal, commercial jet accidents. It is evident that these problems are not restricted to any particular manufacturer, carrier, make, or region of the world. They also demonstrate a need for designing fault detection, identification and Control schemes that actively address faults. These capabilities are important for safety of the passengers and crew.

## 1.2 Background and literature review

A *fault diagnosis system* detects faults, their locations and significance in a system of interest [11]. It normally consists of three tasks: fault detection, fault isolation, and fault identification. A fault in a dynamic system can take on many forms, such as actuator faults, sensor faults, unexpected abrupt changes of some parameters, or even unexpected structural changes [44].

The purpose of fault detection is to generate an alarm which informs the operations that there is at least one fault in the system. This can be achieved by either direct observation of system inputs and outputs or the use of certain types of redundant relations (i.e., analytical redundancy methods). Fault isolation determines the locations of faults, e.g., which sensor or actuator are faulty. Identification, a more difficult task, requires an estimation of the location, size, and nature of the fault [12, 44]. The detection, isolation, and identification tasks are referred to as *fault diagnosis.* Most practical systems contain only fault detection and isolation (FDI).

A traditional approach for fault diagnosis is a hardware-based method in which a particular variable is measured using multiple sensors. Several problems that hardware redundancy based fault diagnosis encounters are the extra equipment, cost, and additional space required to accommodate the redundant equipment [14]. Analytical redundancy is a different approach comparing with the hardware redundancy [16]. A

wide range of analytical redundancy fault diagnosis approaches can be broadly divided into model-based techniques, knowledge-based methodologies, and signal-based techniques [17].

### 1.2.1 Model-Based Fault Diagnosis

In modern fly-by-wire aircraft, hardware redundancy is widely used, where measurements from redundant redundant sensors are compared to each other for fault diagnosis. On the other hand, the sensory measurements in model-based FDI are compared with analytically computed values of the respective variables. The resulting differences, called residuals, are indications of the presence of faults. Parity space [42], parameter estimation and observer-based approach are commonly used methods for model-based residual generation [37].

In recent years, a great deal of methods for robust fault diagnosis have been developed, such as observer-based robust FDI [18, 15, 44], unknown input observers [19, 20, 21], and eigenstructure assignment [23, 24].

The most widely considered method for residual generation are observers. The basic idea is to estimate system's output from the measurements using an observer, and then construct residuals by properly weighted output's estimation errors. When the systems are subject to unknown disturbances and uncertainties, their effect has to be decoupled from the residual signals to avoid false alarms. This problem is well known in the field of FDI as robust fault diagnosis.

Yang and Saif [26] considered a class of special nonlinear systems for FDI purposes. The nonlinear system under consideration can be transformed into two different subsystems. One subsystem uses the adaptive observer canonical form on which an adaptive observer design is based. The other subsystem is affected only by actuator

faults. With the aid of the estimates of states as well as uncertain parameters, the faults are approximated using discretization technique. The approximated faults can be used for fault detection and isolation.

In recent years, a sliding mode observer-based FDI strategy that originated from sliding mode control has been developed [25, 22, 23]. The main point of the SMO is that, despite disturbances and uncertainties, the output estimation errors between the system and the SMO can be forced to and maintained at zero while the system is in sliding regime. Once a fault occurs, sliding will cease to exist, based on this, a failure alarm signal can be generated. Therefore, SMOs are useful for robust FDI.

## 1.3 Organization of the thesis

The rest of the thesis is organized as follows. In Chapter 2, the dynamics of aircraft motion is investigated. A set of generalized nonlinear aircraft equation of motions is given. In Chapter 3, the design of Adaptive Observers (AO) in the case of actuator faults is considered. It is shown that the actuator faults can be adequately addressed by designing appropriate adaptive observers. The design strategy is demonstrated using a model of the Research Civil Aircraft Model Automatic Landing System taken from the literature. In Chapter 4, we consider the design of Sliding Mode Observers (SMOs) for faulty actuators with linear system models. It is shown that the faulty actuators can be rapidly detected and isolated. The details of design are presented in Chapter 4. The necessary and sufficient conditions lead to a novel way to assess the redundancy in systems with regard to actuator faults. Chapter 5 summarizes the work and presents directions for further research. Throughout the thesis, computations are emphasized. Definitions, theorems, and their proofs are relegated to enhance the readability.

# Chapter 2

# The Dynamics of Aircraft Motion

The equation of motion of a rigid body aircraft, moving over the rotating and oblate earth, can be used to delineate the motion of any aerospace vehicle, including satellite and aircraft. For low-speed flight of aircraft flying over a small region of the earth, when there is no requirement for precise simulation of position, it is usual to assume the earth is a flat, inertial frame.

## 2.1 Introduction

The term *rigid body* is an idealistically solid body with finite size in which deformation is neglected. In other words, the distance between any two given points of a rigid body remains constant regardless of external forces exerted on it. The dynamic behavior of the rigid body vehicle can be represented by the force and moment equations as well as the kinematic equations. It is shown that the aerodynamic forces and moments depend on velocity relative to the air mass, with only a weak dependence on altitude [1]. In most cases, this assumption is reasonable for flight simulation and flight-control-system design when it is not necessary to accommodate loads on the aircraft

structure.

The equations of motion will be organized as a set of simultaneous first-order deferential equations with $n$-dimensional variables $x_i$, and $m$-dimensional control input $u_i$. The general form can be expressed as:

$$\begin{aligned} \dot{x_1} &= f_1(x_1, x_2, \cdots, x_n, u_1, \cdots, u_m) \\ &\vdots \\ \dot{x_n} &= f_n(x_1, x_2, \cdots, x_n, u_1, \cdots, u_m) \end{aligned} \tag{2.1}$$

where $f_i$ is a nonlinear and continuous single-valued function, $u_i$ is the control input, and $x_i$'s is the state vector. Eq. (2.1) can be written:

$$\dot{x} = f(x, u), \tag{2.2}$$

where the state vector $X$ is an $n \times 1$ vector, the input vector $U$ is an $m \times 1$ column vector. The nonlinear equations of motion (2.1) or a subset usually have one or more *equilibrium point(s)*. For small perturbations from equilibrium, the Eq. (2.1) are often approximately linear and can be written in matrix form as linear state equations:

$$\dot{x} = Ax + Bu, \tag{2.3}$$

where $x$ and $u$ are the state and control input vectors, $A$ is an $n \times n$ matrix, and $B$ is a $n \times m$ matrix.

## 2.2 Aircraft Coordination System

### 2.2.1 Aircraft Body Axes

When modeling the aircraft or studying aircraft control, it is common to assume that a civil aircraft can be represented as a rigid body, which is defined by a set of body-axis

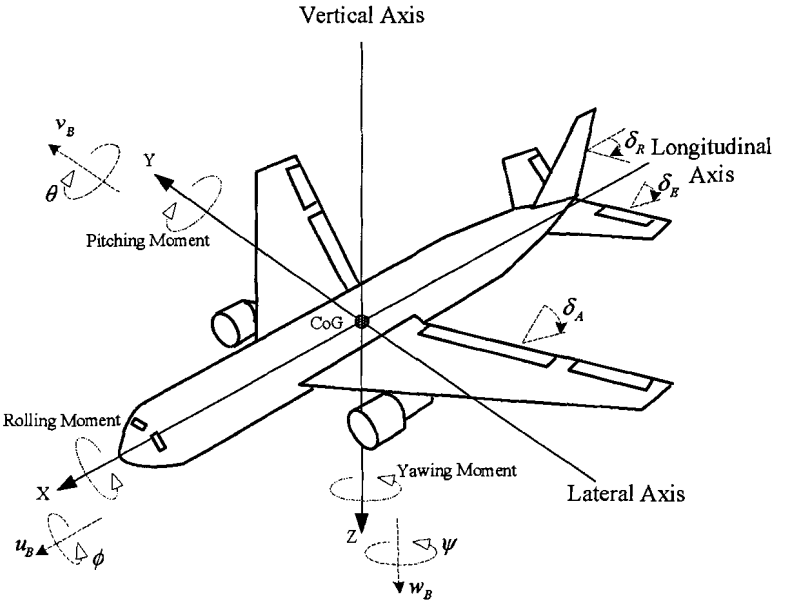


Figure 2.1: Aircraft Rotations - Body Axes

coordinates as shown in Figure 2.1. [27, 28, 29] During filght, it is necessary to control the attitude or orientation of the aircraft in three dimensions, and the aircraft will rotate about its center of gravity(CoG). A three dimensional orthogonal coordinate system is defined through the CoG. Then the orientation of the aircraft is defined by the rotation of the aircraft along its principal axes.

**Yaw** The yaw axis is perpendicular to the plane of the wings with its origin at the CoG and directed towards the bottom of the aircraft. A yaw motion is a movement of the nose of the aircraft from side to side.

**Pitch** The pitch axis is perpendicular to the yaw axis and is parallel to the plane of the wings with its origin at the center of gravity and directed towards the right wing tip. A pitch motion is an up or down movement of the nose of the aircraft.

**Roll** The roll axis is perpendicular to the other two axes with its origin at the CoG, and is directed towards the nose of the aircraft. A rolling motion is an up and

down movement of the wing tips of the aircraft.

During flight, the control surfaces of an aircraft produce aerodynamic forces. These forces are applied to the center of pressure of the control surfaces, which are some distance from the CoG. Accordingly, torques (or moments) about the principal axes cause the aircraft to rotate. The elevators produce pitch moments, the rudder produces yaw moments, and the ailerons produce roll moments. The amount of the forces and moments allows the pilot to maneuver or to trim the aircraft. The first aircraft to demonstrate active control about all three axes was the Wright Brothers' 1902 glider. [1]

The aircraft-body-axis system has its origin at the CoG and orthogonal axes $(x_B, y_B, z_B)$ along the aircraft longitudinal, lateral, and vertical directions respectively, where $x$ is positive forward, $y$ is positive starboard, and $z$ is positive downward. Aircraft body velocities $u_B, v_B, w_B$ are measured along these axes. Variables in the aircraft body axes are denoted by the subscript $B$.

### 2.2.2 Earth Axis System

The earth axis system has its origin at the CoG of aircraft. The $z_E$-axis points vertically downwards; the $x_E$ - axis is always parallel to the earth and points north, and the $y_E$ - axis points east. This coordinate system is usually called North-East-Down (NED) system. Variables in the earth axes system are given the subscript $E$. To transform variables from earth axis to body axis, they are first rotated in roll by an angle $\phi$ (roll angle), in pitch by an angle $\theta$ (pitch angle), and in heading by an angle $\psi$ (heading angle). The relationship between the earth and body axis systems are depicted in Fig. 2.2.

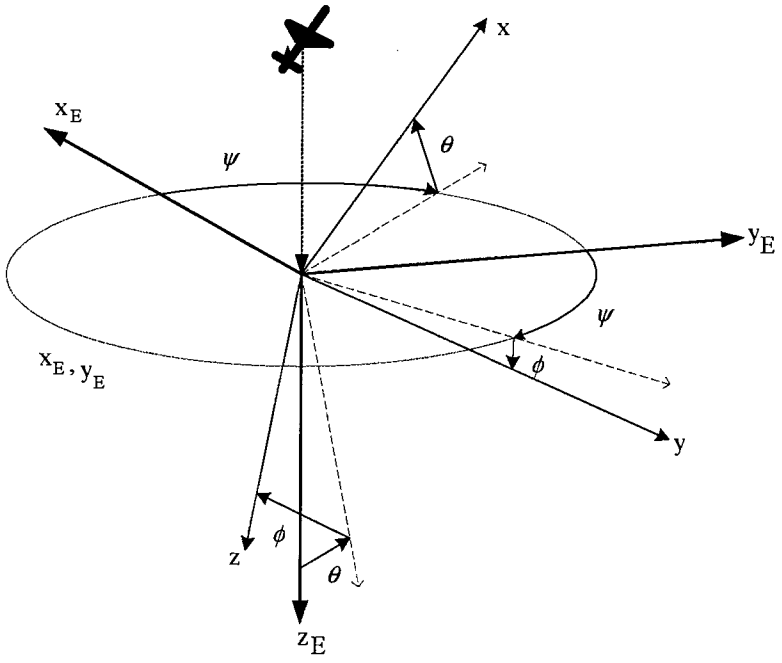


Figure 2.2: Aircraft and Earth Axis System

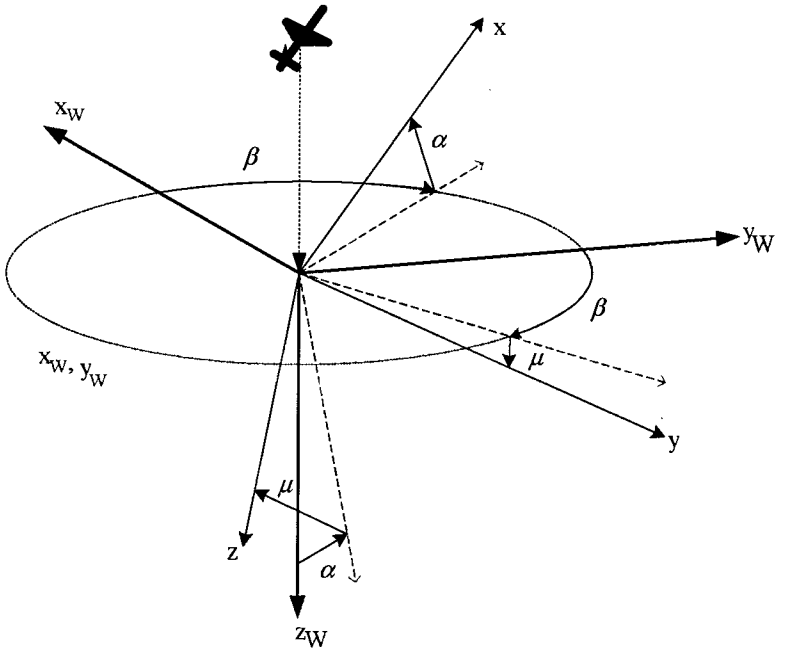


Figure 2.3: Aircraft and Wind Axis System

### 2.2.3 Wind Axis System

The origin of the wind axis system is also located at the CoG. The vector $x_W$ points into the direction of the oncoming free-stream velocity vector, $z_W$ lies in the plane of symmetry of the airplane and is perpendicular to the X-axis and is directed downward, and $y_W$ is perpendicular to both X and Z axes.

To transform variables from wind axes to body axes, they are first rotated in roll by an angle $\mu$ (bank angle), in pitch by an angle $\alpha$ (angle of attack), and in heading by the angle $\beta$ (angle of sideslip). The relationship between the wind and body axis systems are depicted in Fig. 2.3.

The transformation of variables between earth axis and wind axis is only required in two planes. Variables are first rotated in pitch by $\gamma$ (flight path angle) and then in heading by $\chi$ (lateral track angle). The relationship between the earth and wind axis systems are diagrammatically depicted in Fig. 2.4.

### 2.2.4 Flight Control System

The various functions of a generic fly-by-wire flight control computer are shown in Figure 2.5. The flight control computer performs a multitude of functions. It is responsible to translate the pilot commands from the flight cabin (inputs to the pedals, yoke and throttle) to the movement of the control surfaces (ailerons, elevator, flaps, rudder and the actuators for engine speed). The onboard Flight Control Computer (FCC) augments the stability of the aircraft. At the same time, the FCC presents information to the pilot on the various displays, including not only present flight data, but also, weather and navigational information. The FCC is also involved in controlling the communications equipment. It is useful to characterize the function of that the flight control computer into three major categories: safety, performance,

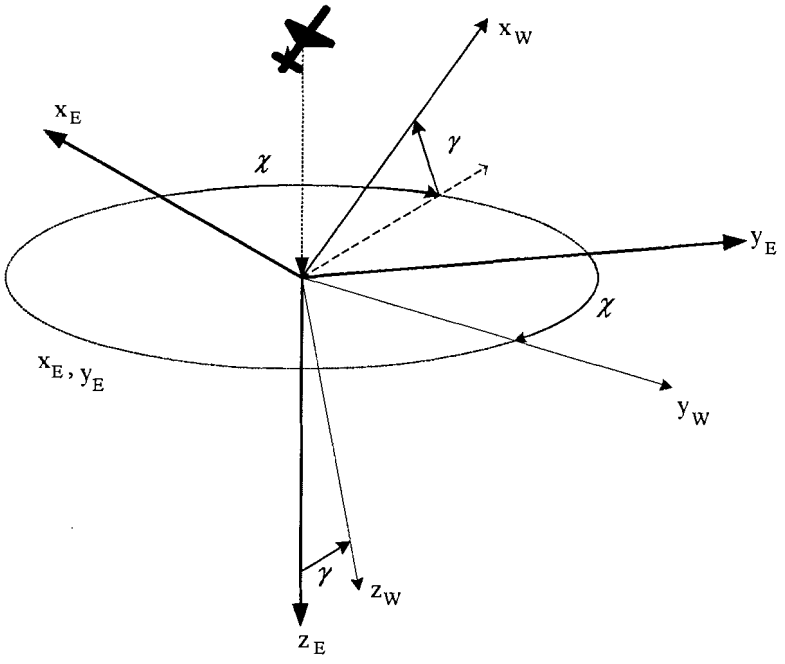


Figure 2.4: Wind and Earth Axis System

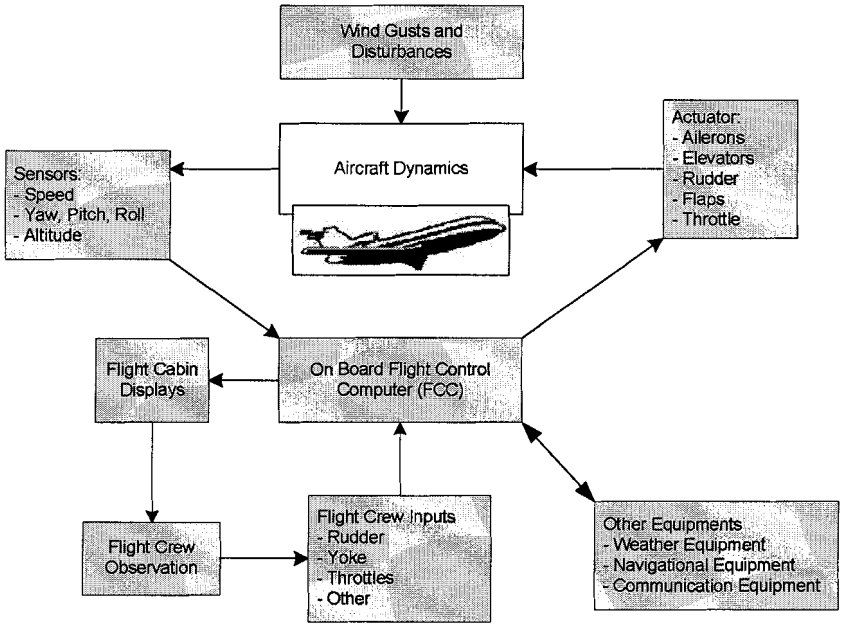


Figure 2.5: Schematics of a Fly-by-wire Aircraft

and comfort.

## 2.3 Forces on An Aircraft

**Weight** Weight is a force that is directed toward the center of the earth. The magnitude of the weight depends on the mass of all the airplane parts, plus the amount of fuel, plus the payload on board (people, baggage, freight, etc.). The weight is distributed throughout the airplane, but it can be viewed as acting through a single point, *CoG*.

Flying of an aircraft encompasses two major problems: Overcoming the weight of an object by some opposing forces, and controlling directions of the object. Both problems are related to the object's weight and the location of its CoG. During flight, the aircraft's weight changes because the aircraft is consuming fuel. The distribution of the weight and the CoG also change. So, the pilot and the control system must constantly adjusts the control inputs to keep the aircraft trimmed.

**Lift** To overcome the weight force, the aircraft has to generate an opposing force, lift. The lift is generated by the motion of the airplane through the air and is an aerodynamic force. Lift is directed perpendicular to the flight direction. Its magnitude depends on several factors including the shape, size, and velocity of the aircraft. Each part of the aircraft contributes to the force of lift, particularly by the wings. The lift acts through a single point called the center of pressure. The center of pressure is defined using the pressure distribution around the body.

$$L = C \times \rho \times \frac{V^2}{2} \times A \tag{2.4}$$

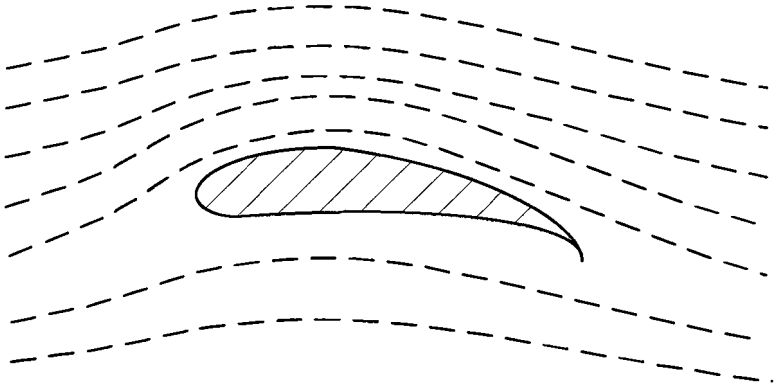

Figure 2.6: Aerodynamic Force - Lift

where $\rho$ is the density of the air, $V$ is the square of the velocity, $A$ the surface area over which the air flows, $C$ is a coefficient determined experimentally. In general, the dependence on body shape, inclination, air viscosity, and compressibility is very complex. The distribution of lift around the aircraft is important for solving the control problem. Aerodynamic surfaces (ailerons, spoilers, rudder, stabilizers, elevators, flaps and slats) are used to control the aircraft in roll, pitch, and yaw.

**Drag** As the aircraft moves through the air, there is another aerodynamic force. The air resists the motion of the aircraft and this resistance force is called drag. The drag is directed along and opposite to the flight direction. Like lift, there are many factors that affect the magnitude of the drag, including the shape of the aircraft, the "stickiness" of the air, and the velocity of the aircraft. All of the individual components' drag force can be combined into a single aircraft drag magnitude, acting through the aircraft center of pressure.

**Thrust** To overcome drag, aircraft use a propulsion system to generate forces called thrust. The direction of the thrust force depends on how the engines are attached

to the aircraft. In Figure 2.1, two turbine engines are located under the wings, parallel to the body, with thrust acting along the body centerline. On some aircraft, such as the Harrier, the thrust directions can be varied to help the airplane take off in a very short distance. The magnitude of the thrust depends on many factors associated with the propulsion system, including the type of engine, the number of engines, and the throttle setting.

For jet engines, the hot gas goes out to the back, so the thrust pushes towards the front. Action reaction is based on by Newton's Third Law of Motion.

The motion of the airplane through the air depends on the relative strength and direction of the forces shown above. If the forces are balanced, the aircraft cruises at a constant velocity. If the forces are unbalanced, the aircraft accelerates in the direction of the largest force.

## 2.4 Aircraft Equation of Motions

### 2.4.1 Definition of Parameters

A six degree of freedom nonlinear model of the Research Civil Aircraft Model (RCAM) has been provided by GARTEUR [54]. The dynamic objects of the RCAM model is shown in 2.7. The inputs to the model are given in Table 2.1 where $F_E$ is the earth-fixed reference frame.

The origin $O_E$ is located on the runway longitudinal axis at the threshold. Frame $x_E$ is positive pointing towards the north, and we assume that the runway is also directed towards the north (runway 00); hence $x_E$ is positive along the runway in the landing direction. Furthermore, $z_E$ is positive downward, and $y_E$ is in the appropriate direction for a right hand coordinate system (positive east). The reference frame $F_B$

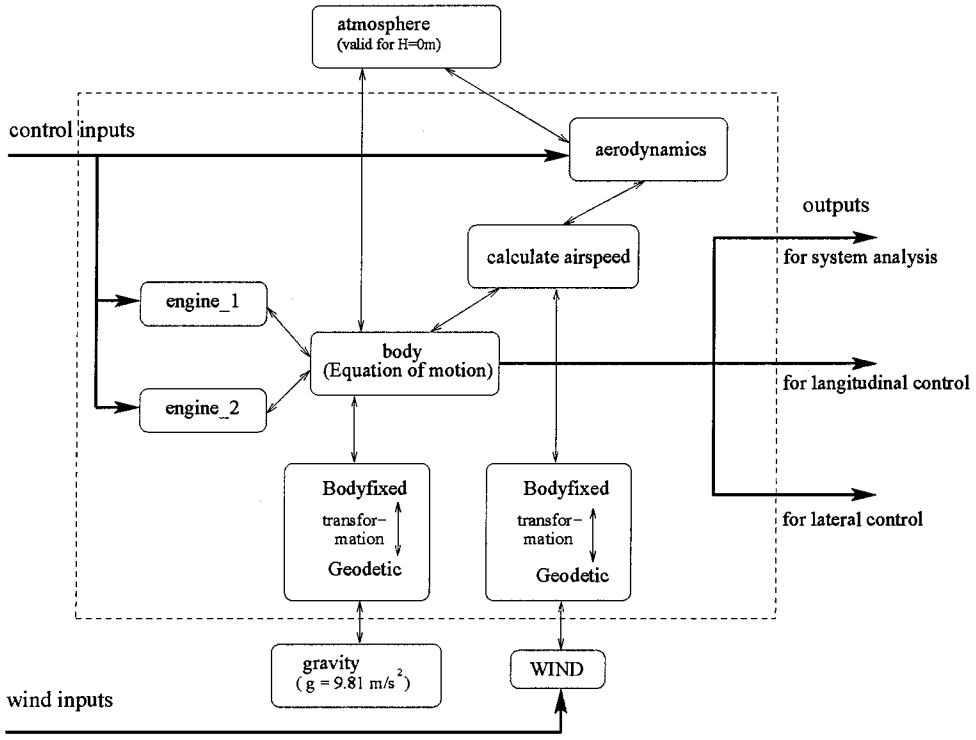


Figure 2.7: Dynamic Objects of RCAM Model

| Symbol | Alphanumeric | | | Name | Unit |
|---|---|---|---|---|---|
| Control inputs | | | | | |
| $\delta_A$ | DA | $u(1)$ | = | aileron deflection | $rad$ |
| $\delta_T$ | DT | $u(2)$ | = | tailplane deflection | $rad$ |
| $\delta_R$ | DR | $u(3)$ | = | rudder deflection | $rad$ |
| $\delta_{TH1}$ | THROTTLE1 | $u(4)$ | = | throttle position of engine1 | $rad$ |
| $\delta_{TH2}$ | THROTTLE2 | $u(5)$ | = | throttle position of engine2 | $rad$ |
| Wind inputs | | | | | |
| $W_{XE}$ | WXE | $u(6)$ | = | wind velocity in the x-axis of $F_E$ | $m/s$ |
| $W_{YE}$ | WYE | $u(7)$ | = | wind velocity in the y-axis of $F_E$ | $m/s$ |
| $W_{ZE}$ | WZE | $u(8)$ | = | wind velocity in the z-axis of $F_E$ | $m/s$ |
| $W_{XB}$ | WXB | $u(9)$ | = | wind velocity in the x-axis of $F_B$ | $m/s$ |
| $W_{YB}$ | WYB | $u(10)$ | = | wind velocity in the y-axis of $F_B$ | $m/s$ |
| $W_{ZB}$ | WZB | $u(11)$ | = | wind velocity in the z-axis of $F_B$ | $m/s$ |

Table 2.1: Model inputs definitions

| Symbol | Alphanumeric | | | Name | Unit |
|---|---|---|---|---|---|
| $p$ | P | $x(1)$ | = | roll rate(in $F_B$) | $rad/s$ |
| $q$ | Q | $x(2)$ | = | pitch rate(in $F_B$) | $rad/s$ |
| $r$ | R | $x(3)$ | = | yaw rate(in $F_B$) | $rad/s$ |
| $\phi$ | PHI | $x(4)$ | = | roll angle(Euler angle) | $rad$ |
| $\theta$ | THETA | $x(5)$ | = | pitch angle(Euler angle) | $rad$ |
| $\psi$ | PSI | $x(6)$ | = | heading angle(Euler angle) | $rad$ |
| $u_B$ | UB | $x(7)$ | = | x component of inertial velocity in $F_B$ | $m/s$ |
| $v_B$ | VB | $x(8)$ | = | y component of inertial velocity in $F_B$ | $m/s$ |
| $w_B$ | WB | $x(9)$ | = | z component of inertial velocity in $F_B$ | $m/s$ |
| $x$ | X | $x(10)$ | = | x position of aircraft CoG in $F_E$ | $m$ |
| $y$ | Y | $x(11)$ | = | y position of aircraft CoG in $F_E$ | $m$ |
| $z$ | Z | $x(12)$ | = | z position of aircraft CoG in $F_E$ | $m$ |

Table 2.2: State Variables Definitions

is body-fixed, defined as bellow.

The origin, $O_B$, is at the CoG, $x_B$ is positive forward, $z_B$ is positive downward, and $y_B$ is positive to the right (starboard side). The three earth-fixed wind inputs, $u(6), u(8)$ are intended to be used for constant wind velocity components, e.g., head-winds. The body-fixed wind inputs are intended to be used for gusts.

The state variables of the model are given in Table 2.2. The outputs of the system are shown in Table 2.3 where $F_V$ is the vehicle-carried vertical frame, which is parallel to the earth-fixed reference frame while moving with the vehicle. The origin, $O_V$, is located on the vehicle's CoG, $x_V$ is positive pointing towards the north, $z_V$ is positive downward, and $y_E$ is positive to the east. For the purpose of simulation, the following outputs are stated in Table 2.4. The model outputs in Table 2.3 can be assumed to be available as inputs to the controller and the observer to be designed. The "simulated outputs" in Table 2.4 are intended to be used for the needs of evaluation. Generally, the inputs, state and output vectors for the body-axes equations can be described as:

| Symbol | Alphanumeric | | | Name | Unit |
|---|---|---|---|---|---|
| $q$ | Q | $y(1)$ | = | pitch rate(in $F_B$) = X(2) | $rad/s$ |
| $n_x$ | NX | $y(2)$ | = | horizontal load factor(in $F_B$) = $F_x/mg$ | - |
| $n_z$ | NZ | $y(3)$ | = | horizontal load factor(in $F_B$) = $F_z/mg$ | - |
| $w_V$ | WV | $y(4)$ | = | $z$ component of inertial velocity in $F_V$ | $m/s$ |
| $z$ | Z | $y(5)$ | = | $Z$ position of the vehicle in $F_E$ =X(12) | $m$ |
| $V_A$ | VA | $y(6)$ | = | airspeed | $m/s$ |
| $V$ | VB | $y(7)$ | = | total inertial airspeed | $m/s$ |
| $\beta$ | BETA | $y(8)$ | = | sideslip angle | $rad$ |
| $p$ | P | $y(9)$ | = | roll rate(in $F_B$) = X(1) | $rad/s$ |
| $r$ | R | $y(10)$ | = | yaw rate(in $F_B$) = X(3) | $rad/s$ |
| $\phi$ | PHI | $y(11)$ | = | roll angle(Euler angle) = X(4) | $rad/s$ |
| $u_V$ | WV | $y(12)$ | = | $x$ component of inertial velocity in $F_V$ | $m/s$ |
| $v_V$ | WV | $y(13)$ | = | $y$ component of inertial velocity in $F_V$ | $m$ |
| $y$ | Y | $y(14)$ | = | y position of aircraft CoG in $F_E$ | $m$ |
| $\chi$ | CHI | $y(15)$ | = | inertial track angle | $rad$ |

Table 2.3: Model Measured Output Definitions

| Symbol | Alphanumeric | | | Name | Unit |
|---|---|---|---|---|---|
| $\theta$ | THETA | $y(16)$ | = | pitch angle(Euler angle) = X(5) | $rad$ |
| $\psi$ | PSI | $y(17)$ | = | heading angle(Euler angle)=X(6) | $rad$ |
| $\alpha$ | ALPHA | $y(18)$ | = | angle of attack(AOA) | $rad$ |
| $\gamma$ | GAMMA | $y(19)$ | = | inertial flight path angle | $rad$ |
| $x$ | X | $y(20)$ | = | x position of aircraft CoG in $F_E$ = X(10) | $m$ |
| $n_y$ | NY | $y(21)$ | = | lateral load factor(in $F_B$) = $F_y/mg$ | - |

Table 2.4: Model Simulation Output Definitions

**Input**

$$U_{Control} = [\delta_A \ \delta_T \ \delta_R \ \delta_{TH1} \ \delta_{TH2}]^T \quad (2.5)$$

$$U_{Wind} = [W_{XE} \ W_{YE} \ W_{ZE} \ W_{XB} \ W_{YB} \ W_{ZB}]^T \quad (2.6)$$

**State**

$$X = [p \ q \ r \ \phi \ \theta \ \psi \ u_B \ v_B \ w_B \ x \ y \ z]^T \quad (2.7)$$

**Output**

$$Y = [q \ n_x \ n_z \ w_V \ z \ V_A \ V \ \beta \ p \ r \ \phi \ u_V \ v_V \ y \ \chi]^T \quad (2.8)$$

$$Y_{Sim} = [\theta \ \psi \ \alpha \ \gamma \ x \ n_y]^T \quad (2.9)$$

Additional inputs can be created when needed for flaps, gear, and spoilers.

### 2.4.2 Six-DOF Nonlinear Model

For the state vector shown in Eq. (2.7), the flat-earth, body-axes 6-degree of freedom Equations of Motion has the following form:

**Force Equation**

$$\begin{aligned} \dot{u_B} &= rv_B - qw_B - g_D sin\theta + (X_A + X_T)/m \\ \dot{v_B} &= -rv_B + pw_B + g_D sin\phi cos\theta + (Y_A + Y_T)/m \\ \dot{w_B} &= qu_B - pv_B + g_D cos\phi cos\theta + (Z_A + Z_T)/m \end{aligned} \quad (2.10)$$

Where $X_T, Y_T, Z_T$ describe the magnitude of the relative wind. $g_D$ is the standard gravity (9.80665 $m/s^2$). $m$ is the mass of the aircraft.

**Kinematic Equations**

$$\begin{aligned} \dot{\phi} &= p + tan\theta(qsin\phi + rcos\phi) \\ \dot{\theta} &= qcos\phi - rsin\phi \\ \dot{\psi} &= (qsin\phi + rcos\phi)/cos\theta \end{aligned} \tag{2.11}$$

**Navigation Equations**

$$\begin{aligned} \dot{x} &= u_B cos\theta cos\psi + v_B(-cos\phi sin\psi + sin\phi sin\theta cos\psi) + w_B(sin\phi sin\psi + cos\phi sin\theta cos\psi) \\ \dot{y} &= u_B cos\theta cos\psi + v_B(cos\phi cos\psi + sin\phi sin\theta sin\psi) + w_B(-sin\phi cos\psi + cos\phi sin\theta sin\psi) \\ \dot{z} &= u_B sin\theta - v_B sin\phi cos\theta - w_B cos\phi cos\theta \end{aligned} \tag{2.12}$$

Normally, civil aircraft spend most of their flying time in a wing-level flight condition. The model of the 3-DOF motion in an NED vertical plane is much simpler than the 6-DOF model. So, it is worth investigating the equations of motion in the wings-level flight condition. In this case, $\phi = 0$, the gravity terms are greatly reduced. Since the angle of side slip is small, the flight path angle is the difference between the aircraft pitch angle and angle of attack, and the gravity terms become:

It can be seen from the kinematic equations in Eq. (2.11), when the roll angle is zero, that:

$$\dot{\theta} = q \tag{2.13}$$

If the roll and yaw rates ($p$ and $r$) are small and the thrust of aircraft is along the axis of $x$, defining $J_Y$ as the inertia of the aircraft on $y$ axis, then the pitch moment is: $\dot{q} = m/J_Y$.

As such, a model for longitudinal motion to the decoupled longitudinal force equations can be obtained with the state vector of $X_l = [\theta\ q\ V\ \alpha]$:

$$\dot{\theta} = q$$

$$\begin{aligned} \dot{q} &= m/J_Y \\ m\dot{V} &= F_T cos(\alpha) - D - mg_D sin(\theta - \alpha) \\ \dot{\alpha}V &= -F_T sin(\alpha) - L + mg_D sin(\theta - \alpha) + Vq \end{aligned} \tag{2.14}$$

With the same scenario, a lateral model can be obtained.

### 2.4.3 Linear Models and Stability Derivatives

The coordinates of a singular point of the implicit nonlinear state-equations are given by a solution, $X = X_e$, which satisfies,

$$f(\dot{X}, X, U) = 0, \quad with\ \dot{X} \equiv 0; U \equiv 0\ or\ constant. \tag{2.15}$$

Steady state flight can be defined as a condition that all the forces and moment components in the body-fixed coordinate system are constant or zero.

$$\dot{p}, \dot{q}, \dot{r},\ and\ \dot{u_B}, \dot{v_B}, \dot{w_B} \equiv 0,\ controls\ fixed \tag{2.16}$$

In the sequel, it is assumed that the mass of aircraft is constant, the aerodynamic angles and the angular rate components are constant and their derivatives are zero. It is also assumed that the flat-earth equations satisfy all system design purposes. The definition allows steady wing-level flight and steady turning flight. In addition, if the change of air density with altitude is negligible, a wing-level climb and a climbing turn can be treated as steady state flight conditions. Therefore, the steady state conditions are important for controller and observer design. Then the steady state flight can be divided into following:

**Steady wing-level flight**

$$\phi = 0, \dot{\phi} = 0, \dot{\theta} = 0, \dot{\psi} = 0;$$

**Steady turning flight**

$$\dot{\phi} = 0, \dot{\theta} = 0, \quad \dot{\psi} = turn\ rate;$$

**Steady Pull up**

$$\phi = 0, \dot{\phi} = 0, \dot{\psi} = 0, \quad \dot{\theta} = pullup\ rate;$$

**Steady Roll**

$$\dot{\theta} = 0, \dot{\psi} = 0, \dot{\phi} = roll\ rate. \tag{2.17}$$

The steady state condition $\dot{p}, \dot{q}, \dot{r}, \equiv 0$ is to regulate the angular rates to be constant or zero, and hence, the aerodynamic and thrust moments must be zero or constant. The conditions of $\dot{u_B}, \dot{v_B}, and \dot{w_B} \equiv 0$ regulate the airspeed, angle of attack, and sideslip to be constant or zero. Therefore, the aerodynamic forces must be zero or constant. The steady state pull-up, and steady state roll-condition, can only exist shortly.

Under ideal situations, the forces acting on an aircraft can produce no-net-external-force. As such, lift is equal to the weight, and the thrust is equal to the drag. A good example of this condition is a cruising airliner. The change of weight due to burned fuel is very small relative to the total aircraft weight. The aircraft maintains a constant airspeed which is called the cruise velocity.

Taking into account the relative velocity of the wind, we can determine the ground speed of a cruising aircraft, which is equal to the airspeed plus the wind speed, by vector addition. The motion of the aircraft is a pure translation. With a constant ground speed, it is relatively easy to determine the aircraft range, which is the distance that the airplane can fly with a given load of fuel.

If the pilot changes the throttle setting, or increases the wing angle of attack, the forces become unbalanced. The aircraft will move in the direction of the greater force. We can compute acceleration of the aircraft from Newton's second law of motion.

If the forces of lift and drag are linearized for small perturbations of a specified flight condition, a set of linear longitudinal equations can be obtained.

In general, as a rigid body moving in a three-dimensional space, an aircraft has a total of six degrees of freedom described by 12 state variables. These variables are divided into four groups:

1. three position variables (position of the aircraft center of gravity CoG),
2. three linear velocity variables (translational velocity of the aircraft CoG),
3. three attitude (orientation) variables,
4. three angular velocity variables.

Aircraft dynamics are normally controlled by four physical inputs: throttle, aileron, elevator, and rudder. The throttle controls the thrust to the aircraft, while the aileron, elevator, and rudder deflections generate aerodynamic forces.

### 2.4.4 Linear RCAM Model

The RCAM [54] is a 6 degree of freedom nonlinear model of a Medium-sized twin-engine aircraft. As shown in Table 2.1, 2.2, 2.3 and 2.4, it combines of 4 inputs, 9 states, 15 measured and 6 simulation outputs. The nonlinear model can be trimmed and linearized at a set of corresponding flight conditions of steady states.

The flight condition of a wing-level steady state is chosen to be linearized for the controller and observer design in the following chapters.

- Airspeed 80 $m/s$
- Altitude 305 $m$ (1000 feet)
- Aircraft Mass 120 $Tonnes$
- Flight Path Angle 0° (level)
- Still air (no wind effects)

**Longitudinal Model** For longitudinal model, the airspeed $V_A$ and altitude $z$ are kept at trim condition. The changes in pitch rate $q$, vertical acceleration $n_Z$, and vertical velocity $w_E$ need to be regulated.

The linear RCAM longitudinal model with two inputs, five outputs, and five states, can be in the form of:

$$\begin{aligned} \dot{x} &= Ax + Bu \\ y &= Cx \end{aligned} \tag{2.18}$$

$$A_{long} = \begin{bmatrix} -0.98 & 0 & 0 & -0.016 & 0 \\ 1.00 & 0 & 0 & 0 & 0 \\ -2.190 & -9.780 & -0.028 & 0.074 & 0 \\ 77.360 & -0.770 & -0.220 & -0.670 & 0 \\ 0 & -79.97 & -0.03 & 0.99 & 0 \end{bmatrix}, \quad B_{long} = \begin{bmatrix} -2.44 & 0.58 \\ 0 & 0 \\ 0.180 & 19.620 \\ -6.480 & 0 \\ 0 & 0 \end{bmatrix},$$

$$C_{long} = \begin{bmatrix} 1 & 0 & 0 & 0 & 0 \\ 7.88 & -0.078 & -0.023 & -0.068 & 0 \\ 0 & 0 & 0.99 & 0.029 & 0 \\ 0 & -79.97 & -0.028 & 0.99 & 0 \\ 0 & 0 & 0 & 0 & 1 \end{bmatrix}$$

The inputs($u$), states($x$), outputs(y) variables of the linear longitudinal model are defined in Table 2.1, 2.2, 2.3 and 2.4, where

$$x_{long} = [q\ \theta\ u_B\ w_B\ z]^T$$

$$\begin{aligned} y_{long} &= [q\ n_Z\ V_A\ w_E\ z]^T \\ u_{long} &= [\delta_t\ \delta_{th}]^T \end{aligned} \tag{2.19}$$

**Lateral Model** For the lateral model, the heading rate $\psi$ and lateral displacement *ylat* needs to be regulated. Side-slip angle $\beta$, roll rate $p$, yaw rate $r$, and track angle $\chi$ are chosen as output signals for the purpose of control and fault diagnosis during an engine failure. As the regulation of lateral deviation, *ylat* is a necessary part of the controller.

The linear RCAM lateral model with two inputs, five states and five outputs can be shown as the same form of Eq. (3.18),

$$A_{lat} = \begin{bmatrix} -1.270 & 0.550 & 0 & 0 & -0.024 \\ 0.052 & -0.502 & 0 & 0 & 0.005 \\ 1.000 & 0.028 & 0 & 0 & 0 \\ 0 & 1.000 & 0 & 0 & 0 \\ 2.270 & -79.00 & 9.970 & 0 & -0.170 \end{bmatrix}, \quad B_{lat} = \begin{bmatrix} -0.840 & 0.290 \\ -0.018 & -0.330 \\ 0 & 0 \\ 0 & 2.038 \\ 0 & 0 \end{bmatrix},$$

$$C_{lat} = \begin{bmatrix} 0 & 0 & 0 & 0 & 0.013 \\ 1.000 & 0 & 0 & 0 & 0 \\ 0 & 1.000 & 0 & 0 & 0 \\ 0 & 0 & 1.000 & 0 & 0 \\ 0 & 0 & -0.028 & 1.000 & 0.013 \end{bmatrix}$$

The inputs($u$), states($x$), outputs(y) variables of the linear lateral model are defined in Table 2.1, 2.2, 2.3 and 2.4, where

$$\begin{aligned} x_{lat} &= [p\ r\ \phi\ \psi\ v_B]^T \\ u_{lat} &= [\delta_a\ \delta_r]^T \\ y_{lat} &= [\beta\ p\ r\ \phi\ \chi]^T \end{aligned} \tag{2.20}$$

# Chapter 3

# Adaptive Observer For Actuator FDI

This chapter is concerned with the problem of detecting and isolating the actuator faults using an adaptive observer (AO). Two AOs were constructed. One AO uses system states and inputs, and another one uses only system outputs and inputs for diagnosing actuator faults. The construction of this observer is based on the linear system. Sufficient conditions for the proposed observer is proved. This makes the calculation of the observer gain matrix easier. It is shown that the proposed approach is robust in the sense that the residual will only produce an alarm only after a fault occurs.

## 3.1 Introduction

Many efforts have been made towards observer-based approaches to fault diagnosis. [39, 44, 52, 63] For a deterministic system, The basic idea behind this approach is to use an observer to estimate system outputs from measurements by employing a

Luenberger observer. In this case, output estimation errors can be taken as residuals.

Once a fault is successfully detected, its location has to be found. This is the task of fault isolation and it is very crucial for fault accommodation. More results have been reported on fault detection than on fault isolation although fault isolation (usually more difficult than fault detection) has not been completely solved refer to related references in survey papers by Willsky [36], Iserman [37], Gertler [38], Frank [39], Patton [41], and Fank [42] for details.

To isolate faults, two schemes based on banks of observers have been proposed. One is called *dedicated observer scheme* as proposed by Clark [52]. In this scheme, to isolate a fault among $N$ possible faults, $N$ observers generate $N$ residuals and the $i$th residual is only sensitive to the $i$th fault but decoupled from all other faults. it can detect and isolate several faults, robustness against parameter uncertainties but no robustness against unknown inputs. The "non-robustness" lies on the fact that only one measurement as observer input is used. This scheme can only be used to detect and isolate a single fault [13].

The other scheme is the *generalized observer scheme* by Frank [39]. In this latter method, $N$ observers generate $N$ residuals. However, the $i$th residual is sensitive to all other faults except the $i$th fault. Therefore, this scheme provides more freedom in the observer design especially to increase the robustness on parameter variations or unknown inputs in the system. We have adopted the generalized observer scheme to achieve multi faults isolation.

In observer-based fault detection, a full or reduced order observer is applied for the residual generation. Subsequently, fault detection becomes an equivalent state space feedback control problem because there are dual relations between the observer design and the state feedback control.

Zhang et al. [48] proposed a method which can be used for robust actuator fault isolation. To apply this scheme, all states must be available and known. Wang and Daley [44] introduced an approach for fault detection and isolation in which faults can be represented by the product of an constant unknown parameters matrix and the system input. To obtain accurate parameter estimation, the excitation signals may be needed. Chen and Saif [43] introduced an adaptive robust actuator fault isolation scheme. This scheme can be used either when all states are available or only the outputs are available.

In this chapter, using adaptive observers, constant actuator fault isolation problems for a class of linear systems were investigated. Sufficient actuator fault isolation conditions are derived for the case that all states are measured and the case that only outputs are available. Based on Research Civil Aircraft Model (RCAM), simulation examples are given to show the effectiveness of our schemes in aircraft actuator fault detection and isolation .

## 3.2 Actuator Fault Isolation with Adaptive Observers

In this section, the actuator fault isolation schemes were designed for a class of linear systems. Two cases were investigated. One is that all states are available. Another case is that only outputs are available. Sufficient conditions for actuator fault isolation are given for the two cases.

### 3.2.1 Case I: State Vector is Measurable

Consider the following linear system,

$$\dot{x} = Ax + Bu \tag{3.1}$$

where $x \in R^n$ is the state vector, $u \in R^m$, the output of actuators, is the input vector. The $n \times m$ the matrix $B$ is the distribution matrix of the actuators.

In this chapter, it is assumed that only actuator faults can occur. Define $u_j^f(t) \equiv u_j^f$ for $t \geq t_f$ and $\lim_{t\to\infty} |u_j(t) - u_j^f| \neq 0$, $u_j^f$ is a faulty constant output of $j$th actuator, where $j \in 1, 2, \ldots, m$ and $u_j(t)$ is the $j$th healthy actuator output.

**Remark 3.2.1** In aircraft control systems, constant actuator faults often occur [47, 49].

In this chapter, we consider the following fault detection and isolation problem:

It is desired to design an observer based scheme to isolate the faulty actuator when faults have occurred.

An adaptive observer based scheme was utilized to isolate the faulty actuator. For simplicity, only one single actuator fault at a time is considered. Multiple faulty actuators can be treated by extending the proposed method.

Fault detection can be achieved because all states are available. Fault detection is achieved by comparing the actual system state observations to the measured model states. If any actual system state is not acting as desired, it can be concluded that faults have occurred in the actual system. The remaining question is determine which actuator is faulty.

Since the system (3.1) has $m$ inputs corresponding to $m$ sets of actuators, there are $m$ possible fault models for the actuator. Assuming the $l$th actuator is faulty, the

corresponding fault model is:

$$\begin{aligned} \dot{x} &= Ax + \sum_{j \neq l} b_j u_j + b_l u_l^f(t) \\ &= Ax + \sum_{j \neq l} b_j u_j + b_l u_l^f \end{aligned} \tag{3.2}$$

where $B = (b_1|\cdots|b_l|\cdots|b_m)$ and $b_l$ is the column vector of $B$.

A bank of observers can be designed for the possible fault models using the following adaptation techniques,

$$\begin{aligned} \dot{\hat{x}}_i &= H(\hat{x}_i - x) + Ax + \sum_{j \neq i} b_j u_j + b_i \hat{u_i^f} \\ \dot{\hat{u_i^f}} &= -2\gamma e_{x_i}^T P b_i \end{aligned} \tag{3.3}$$

where $1 \leq i \leq m$ and $e_{x_i} = \hat{x}_i - x$, $H$ is a Hurwitz matrix which can be chosen freely, and $\gamma$ is a design constant. $P$ is a positive definite matrix which is a solution of the following matrix equation:

$$H^T P + PH = -Q \tag{3.4}$$

where $Q$ is a positive definite matrix. Then, the following results can be found.

*Theorem 2.1*: If the $l$th actuator is faulty, when $i = l$ it can be shown:

$$\lim_{t \to \infty} e_{x_l} = 0$$

and for $i \neq l$,

$$\dot{e}_{x_i} = He_{x_i} + b_l(u_l - u_l^f) - b_i(u_i - \tilde{u_i^f}) \tag{3.5}$$

*Proof of Theorem 2.1*:

- For $i = l$, from Eqs. (3.2) and (3.3):

$$\dot{e}_{x_l} = He_{x_l} + b_l \tilde{u_l^f} \tag{3.6}$$

Choose a Lyapunov function:

$$V = e_{x_l}^T P e_{x_l} + \frac{1}{2\gamma}(\tilde{u_l^f})^2 \tag{3.7}$$

where $\tilde{u_l^f} = \hat{u_l^f} - u_l^f$. Differentiate Eq. (3.7) with respect to $t$, from Eq. (3.6) and (3.3):

$$\begin{aligned} \dot{V} &= -e_{x_l}^T Q e_{x_l} + \frac{1}{\gamma}(\tilde{u_l^f})[(\dot{u_l^f}) + 2\gamma(e_{x_l})^T P b_l] \\ &= -e_{x_l}^T Q e_{x_l} \\ &\leq 0 \end{aligned} \tag{3.8}$$

From the above result, it can be shown that

$$\lim_{t\to\infty} e_{x_l} = 0.$$

- For $i \neq l$, the fault model is:

$$\dot{x} = Ax + \sum_{j\neq i,l} b_j u_j + b_i u_i + b_l u_l^f \tag{3.9}$$

At this time, the $i$th observer is:

$$\begin{aligned} \dot{\hat{x}}_i &= H(\hat{x}_i - x) + Ax + \sum_{j\neq i,l} b_j u_j + b_l u_l + b_i \hat{u_i^f} \\ \dot{\hat{u_i^f}} &= -2\gamma(e_{x_i})^T P b_i \end{aligned} \tag{3.10}$$

Thus,

$$\dot{e}_{x_i} = He_{x_i} + b_l(u_l - u_l^f) - b_i(u_i - (\hat{u_i^f})) \tag{3.11}$$

This completes the proof. ★

The residuals can be defined as $r_i(t) = ||e_{x_i}(t)||^2$ for $1 \leq i \leq m$. Monitoring all residuals, $[r_1(t), \cdots, r_l(t), \cdots, r_m(t)]$, it can be concluded that, if there is a $l$, $1 \leq l \leq m$, such that $\lim_{t\to\infty} r_l(t) = 0$ with $\lim_{t\to\infty} r_i(t) \neq 0$ for all $i \neq l$, then the $l$th actuator is faulty.

To find when the above condition can be applied, a sufficient condition for the actuator isolation is shown as follow:

*Theorem 2.2*: If matrix $B$ is of full column rank, fault actuator isolation can be achieved by measuring the residuals from Eq. (3.3).

*Proof of Theorem 2.2*: From Theorem 2.1, when an actuator fault occurs, the residual corresponding to the fault model, $r_l(t)$, will go to zero. We need to prove all other residual that is $i \neq l$ do not tend to zero.

- For any $i \neq l$, $b_i$ and $b_l$ are independent because $B$ is of full column rank, which is $b_l(u_l - u_l^f) - b_i(u_i - \hat{u_i^f})$ is nonzero for all $t$ if $u_l - u_l^f \neq 0$. Together with $\lim_{t\to\infty} |u_l - u_l^f| \neq 0$, we conclude that

$$\lim_{t\to\infty} b_l(u_l - u_l^f) - b_i(u_i - \hat{u_i^f}) \neq 0$$

  where $i \neq l$. Thus $r_i(t)$ will not go to zero for any $i \neq l$. This completes the proof. ★

**Remark 3.2.2** Theorem 2.2 presents a sufficient condition for fault isolation. If the distribution matrix of the actuators $B$ does not have full column rank, we cannot conclude that the fault cannot be isolated. Although the fault may not be isolated using this approach, other methods could be used.

### 3.2.2 Case II: Only the Output Vector is Measurable

Consider the linear system,

$$\dot{x} = Ax + Bu$$

$$y = Cx \tag{3.12}$$

where $x \in R^n$ is the state vector, $u \in R^m$ is the input vector, and $y \in R^q$ is the outputs. In most practical applications, only the output $y$ is available. The methods discussed in section 3.2.1 cannot be used because $e_x$ is no longer available.

To design a fault isolation observer, the following assumption is needed, which is the same as the assumption for the sliding mode observer utilized in Chapter 4.

Assumption $A1$: There exist positive definite matrices $P$, $Q$ and matrices $L$, $F$ such that

$$\begin{aligned} (A-LC)^T P + P(A-LC) &= -Q \\ PB &= C^T F^T \end{aligned} \tag{3.13}$$

To find $P$, $Q$, $L$ and $D$, the algorithm of references [59, ?] can be used.

In Section 3.2.1, a fault actuator model is given. For the system represented by Eq. (3.12), if the $l$th actuator is faulty, the corresponding fault model is:

$$\begin{aligned} \dot{x} &= Ax + \sum_{j \neq l} b_j u_j + b_l u_l^f \\ y &= Cx \end{aligned} \tag{3.14}$$

A bank of observers can be designed for the fault models as follows:

$$\begin{aligned} \dot{\hat{x}}_i &= A\hat{x}_i - L(\hat{y}_i - y) + \sum_{j \neq i} b_j u_j + b_i(\hat{u_i^f}) \\ \dot{\hat{u_i^f}} &= -2\gamma (e_{y_i})^T f_i \end{aligned} \tag{3.15}$$

where $1 \leq i \leq m$, $\hat{y}_i = C\hat{x}_i$ and $e_{y_i} = \hat{y}_i - y = Ce_{x_i}$, $\gamma$ is a design constant, and $P$, $Q$, $L$ and $F^T = (f_1, \cdots, f_m)$ satisfy Eq. (3.13).

*Theorem 2.3*: If the $l$th actuator is faulty, when $i = l$,

$$\lim_{t \to \infty} e_{x_i} = \lim_{t \to \infty} e_{x_l} = 0. \tag{3.16}$$

and for all $i \neq l$,

$$\dot{e}_{x_i} = (A - LC)e_{x_i} + b_l(u_l - u_l^f) - b_i(u_i - \hat{u_i^f}) \tag{3.17}$$

From the *dedicated observer scheme*, the residual is defined as $r_i(t) = ||e_{y_i}(t)||^2$ where $1 \leq i \leq m$. Monitoring all residuals, $[r_1(t), \cdots, r_l(t), \cdots, r_m(t)]$, it can be concluded that, if there exist a $l$ $(1 \leq l \leq m)$, when the system satisfies $\lim_{t\to\infty} r_l(t) = 0$ while $\lim_{t\to\infty} r_i(t) \neq 0$ for all $i \neq l$, the $l$th actuator is faulty. This completes the fault isolation of the $l$th actuator.

According to the above criterion, a sufficient condition for actuator isolation is given bellow:

*Theorem 2.4*: If the matrix $CB$ has full column rank, the fault actuator isolation can be achieved by measuring the residuals from the observer described by Eq. (3.15) based on Assumption A1.

*Proof of Theorem 2.4*: When a fault occurs, we know that $e_{x_l}$ will tend to zero. The residual corresponding to the fault model, $r_l(t)$, will go to zero too. Define $T_i(s) = C[sI-(A-LC)]^{-1}b_i$, $1 \leq i \leq l$. For any $i \neq j$, $T_i(s)$ and $T_j(s)$ are independent because $Cb_i$ and $Cb_j$ are independent. Then $r_i(t) = G_l(s)(u_l - u_l^f) - G_i(s)(u_i - \hat{u_i^f})$ will not tend to zero because $u_l - \lambda_l$ will not tend to zero. Thus, for all $i \neq l$, $r_i(t)$ does not tend to zero. This completes the proof. ★

**Remark 3.2.3** Theorem 2.4 presents a sufficient condition for fault isolation. The condition that $CB$ has full column rank is a natural extension of the preceding condition that $B$ has full rank. If $CB$ does not have full column rank, we cannot conclude that the fault cannot be isolated. The fault may not be isolated using this approach, however, other methods could be used.

## 3.3 Simulation results

In this section, applying the longitudinal and lateral RCAM models, we consider the two cases of systems to show the effectiveness of the proposed fault isolation schemes. In all simulations, we assume that the actuator has a constant fault at time 4.00 sec.. The fault isolation observers run simultaneously with the real systems.

We consider a system of longitudinal and lateral RCAM models as described in Chapter. 2. For convenience, we repeat the models as follows:

$$\begin{aligned} \dot{x} &= Ax + Bu \\ y &= Cx \end{aligned} \tag{3.18}$$

### 3.3.1 Longitudinal Model

$$A_{long} = \begin{bmatrix} -0.98 & 0 & 0 & -0.016 & 0 \\ 1.00 & 0 & 0 & 0 & 0 \\ -2.190 & -9.780 & -0.028 & 0.074 & 0 \\ 77.360 & -0.770 & -0.220 & -0.670 & 0 \\ 0 & -79.97 & -0.03 & 0.99 & 0 \end{bmatrix}, \quad B_{long} = \begin{bmatrix} -2.44 & 0.58 \\ 0 & 0 \\ 0.180 & 19.620 \\ -6.480 & 0 \\ 0 & 0 \end{bmatrix},$$

$$C_{long} = \begin{bmatrix} 1 & 0 & 0 & 0 & 0 \\ 7.88 & -0.078 & -0.023 & -0.068 & 0 \\ 0 & 0 & 0.99 & 0.029 & 0 \\ 0 & -79.97 & -0.028 & 0.99 & 0 \\ 0 & 0 & 0 & 0 & 1 \end{bmatrix}$$

with

$$\begin{aligned} x_{long} &= [q\ \theta\ u_B\ w_B\ z]^T \\ y_{long} &= [q\ n_Z\ V_A\ w_E\ z]^T \\ u_{long} &= [\delta_t\ \delta_{th}]^T \end{aligned} \tag{3.19}$$

The longitudinal control objective is to design a feedback controller to make the state vector $x$ stay at

$$b = [0, \quad 0.0678, \quad 79.98, \quad 0.861, \quad 305]^T$$

To realize the above control goal, the following feedback controller is designed:

$$\begin{aligned} x &= C^{-1}y \\ u &= -K(x-b) + u_c \end{aligned} \tag{3.20}$$

where $K$ is chosen such that the closed-loop poles are assigned at

$$K_{long} = [-1, \quad -2, \quad -0.5, \quad -0.3, \quad -1.5]$$

and $u_c = (\,0.1865 \quad 0.009\,)^T$ is a solution of $Ab + Bu = 0$.

If there are no faults, this controller can indeed drive the system state vector to $b$ asymptotically. Denoting $B = [B1 \;\; B2]$, $K = \begin{bmatrix} K1 \\ K2 \end{bmatrix}$, it can be verified that both $A - B1K1$ and $A - B2K2$ are Hurwitz matrices. This is necessary for the case when the actuator faults might occur.

It can be shown that $\lim_{t\to\infty} x(t) = 0$ if the actuators are healthy. Choose $L$ to assign the poles of $A - LC$ at

$$P_{longob} = [-1, \quad -3, \quad -1.5, \quad -10, \quad -2.5].$$

For the case that the states are available, set $P = I$ and $Q = I$, then Eq. (3.4) is satisfied.

The observers are designed as follows:

$$\begin{aligned} \dot{\hat{x}}_1 &= H(\hat{x}_1 - x) + Ax + b_2u_2 + b_1\hat{u_1^f} \\ \dot{\hat{u_1^f}} &= -2\gamma e_{x_1}^T P b_1 \end{aligned} \tag{3.21}$$

and

$$\begin{aligned} \dot{\hat{x}}_2 &= H(\hat{x}_2 - x) + Ax + b_1 u_1 + b_2 \hat{u_2^f} \\ \dot{\hat{u}}_2^f &= -2\gamma e_{x_2}^T P b_2 \end{aligned} \tag{3.22}$$

For the case that only the output is available, set $P = I_{5\times 5}$. Then

$$D = \begin{bmatrix} -750.7479 & 94.9629 & 2.3854 & -0.0926 & 0 \\ -65.7353 & 8.4157 & 20.0135 & -0.0082 & 0 \end{bmatrix},$$

The observers are designed as follows

$$\begin{aligned} \dot{\hat{x}}_1 &= A\hat{x}_1 - L(\hat{y}_1 - y) + b_2 u_2 + b_1 \hat{u_1^f} \\ \dot{\hat{u}}_1^f &= -2\gamma (e_{y_1})^T f_1 \end{aligned} \tag{3.23}$$

and

$$\begin{aligned} \dot{\hat{x}}_2 &= A\hat{x}_2 - L(\hat{y}_2 - y) + b_1 u_1 + b_2 \hat{u_2^f} \\ \dot{\hat{u}}_2^f &= -2\gamma (e_{y_2})^T f_2 \end{aligned} \tag{3.24}$$

It can be verified that Eq. (3.13) is satisfied. The fault isolation observers can be designed using the approach of Eq. (3.3). Since $A_L = A - LC$ is symmetric, $e^{A_L t}$ is positive definite for any $t$. Since $B$ and $C$ has full column rank, $Ce^{A_L t}$ has full column rank for any $t$. From the sufficient condition we derived for this case, we conclude that constant actuator fault isolation can be accomplished. The fault isolation method has been simulated for the longitudinal model with $x(0) = (0.0000,\ \ 0.0400,\ \ -8.5844,\ \ 2.9688,\ \ -1.8231)^T$ and other initial values are all set to zero, and $\rho = 1$. From Figs. 3.1-3.4, it can be seen that the faulty residual $r_i(t)$ goes to zero while the healthy residual $r_l(t)$ does not.

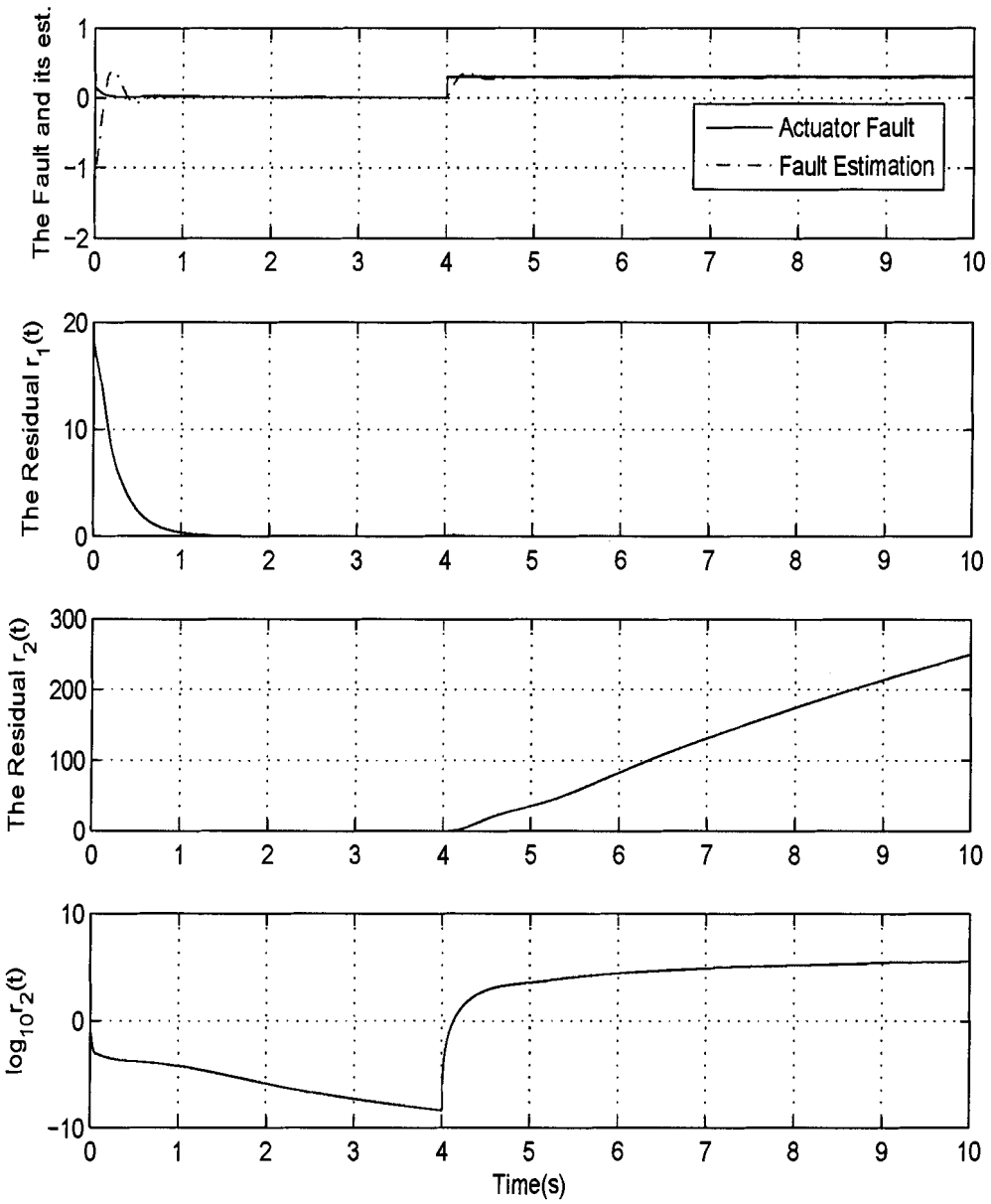


Figure 3.1: Actuator 1's fault estimation with full state measurable - longitudinal model

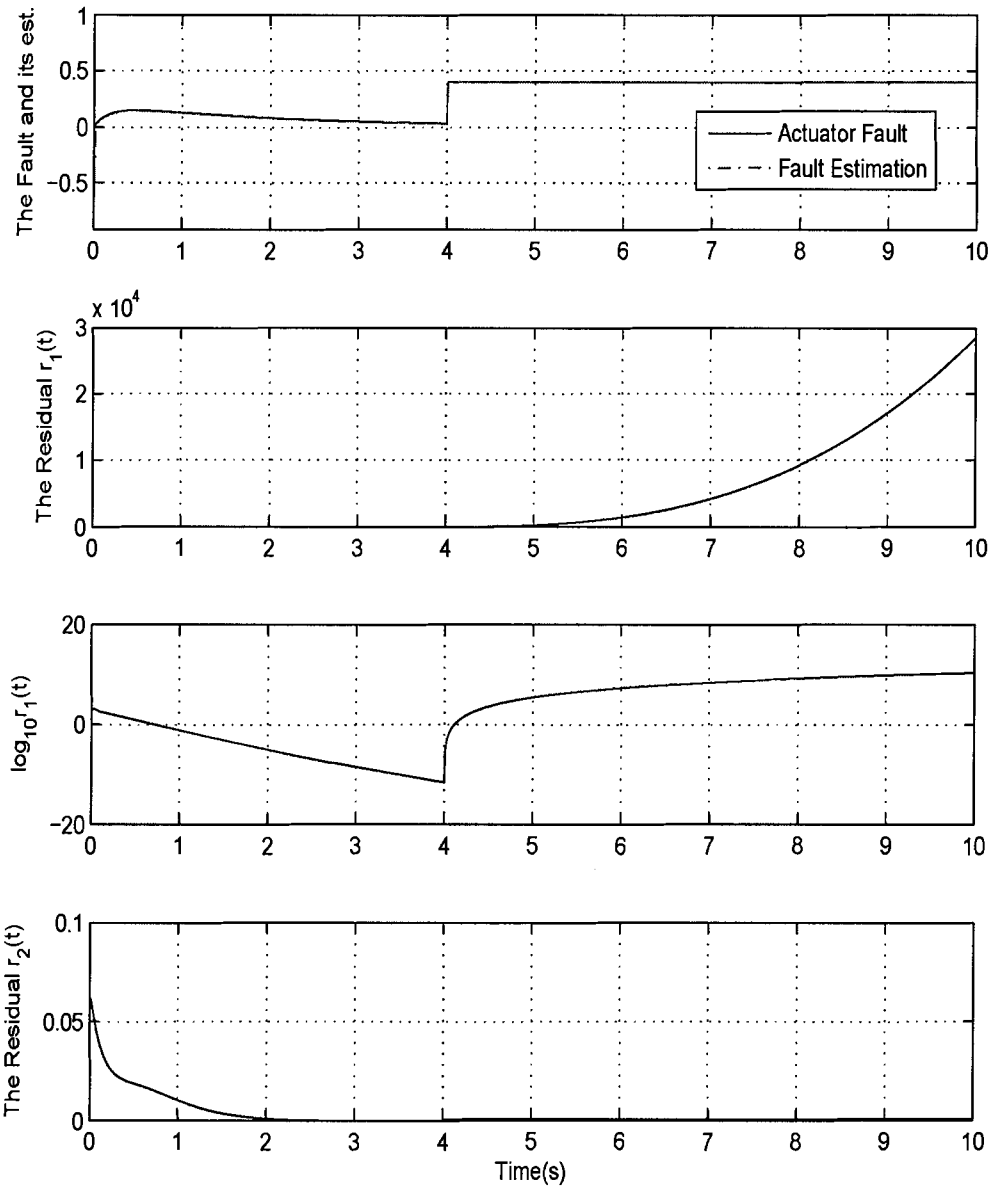


Figure 3.2: Actuator 2's fault estimation with full state measurable - longitudinal model

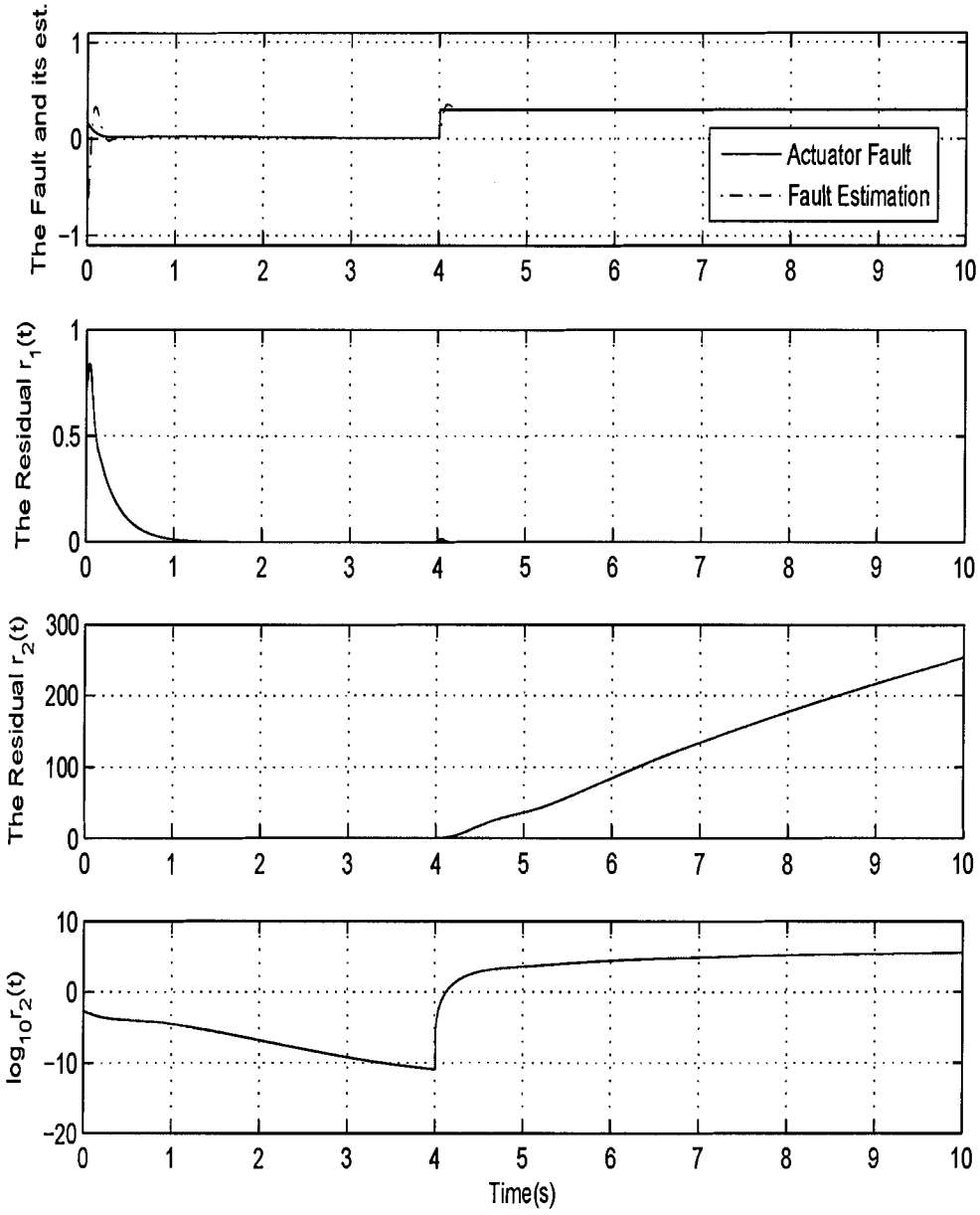


Figure 3.3: Actuator 1's fault estimation with only output measurable - longitudinal model

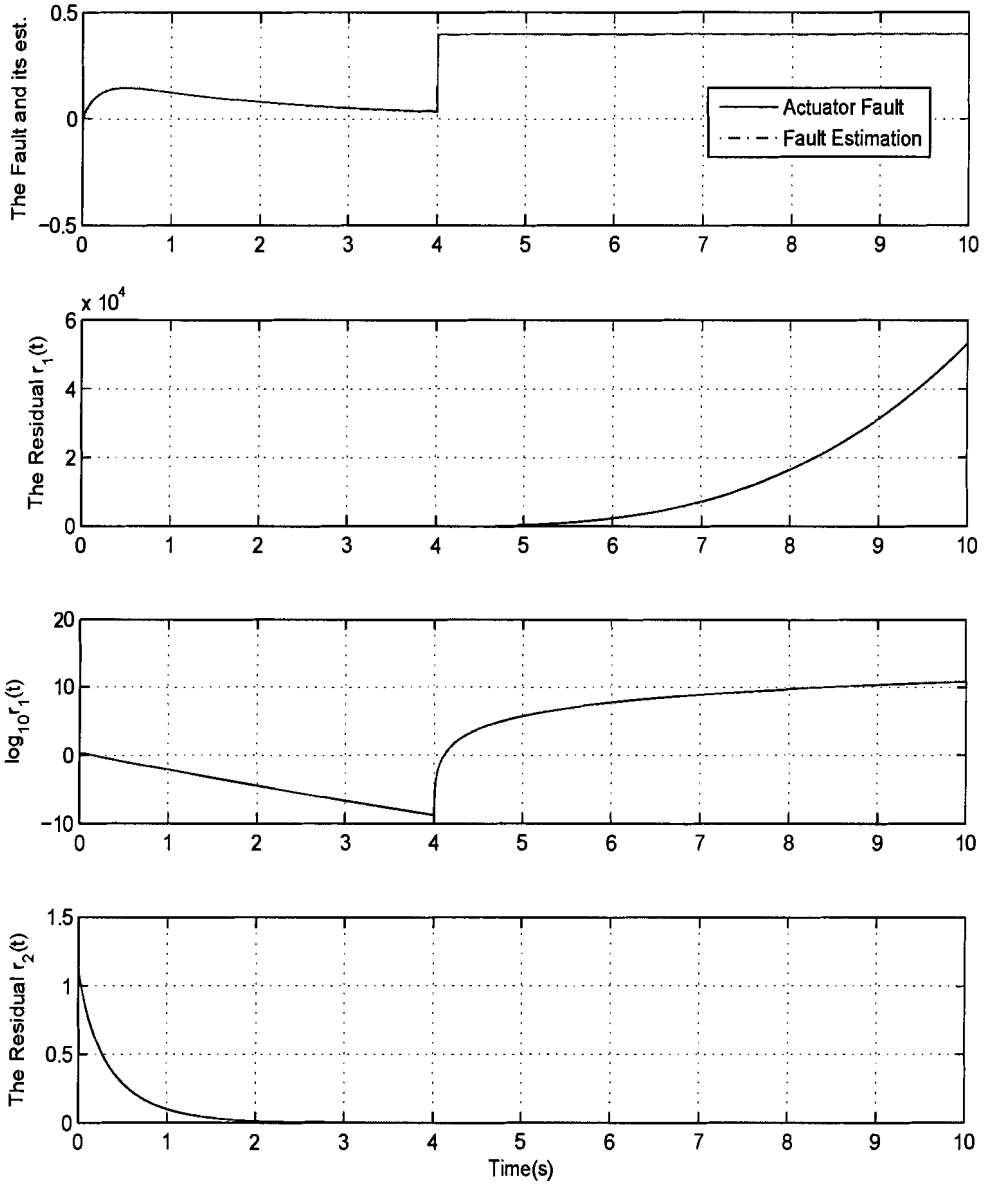


Figure 3.4: Actuator 2's fault estimation with only output measurable - longitudinal model

### 3.3.2 Lateral Model

$$A_{lat} = \begin{bmatrix} -1.270 & 0.550 & 0 & 0 & -0.024 & 0 \\ 0.052 & -0.502 & 0 & 0 & 0.005 & 0 \\ 1.000 & 0.028 & 0 & 0 & 0 & 0 \\ 0 & 1.000 & 0 & 0 & 0 & 0 \\ 2.270 & -79.00 & 9.970 & 0 & -0.170 & 0 \\ 0 & 0 & 0 & 0 & 0 & 1 \end{bmatrix}, \quad B_{lat} = \begin{bmatrix} -0.840 & 0.290 \\ -0.018 & -0.330 \\ 0 & 0 \\ 0 & 2.038 \\ 0 & 0 \\ 0 & 0 \end{bmatrix},$$

$$C_{lat} = \begin{bmatrix} 0 & 0 & 0 & 0 & 0.013 \\ 1.000 & 0 & 0 & 0 & 0 \\ 0 & 1.000 & 0 & 0 & 0 \\ 0 & 0 & 1.000 & 0 & 0 \\ 0 & 0 & -0.028 & 1.000 & 0.013 \\ 0 & 0 & -2.260 & 79.87 & 1.000 \end{bmatrix}$$

with

$$\begin{aligned} x_{lat} &= [p \ r \ \phi \ \psi \ v_B \ y_p]^T \\ u_{lat} &= [\delta_a \ \delta_r]^T \\ y_{lat} &= [\beta \ p \ r \ \phi \ \chi \ y_p]^T \end{aligned} \tag{3.25}$$

The lateral control objective is to design a feedback controller to make the state vector $x$ stay at the neutral position which is $b = [0,\ 0,\ 0,\ 0,\ 0,\ 0,]^T$. The feedback gain is chosen as $K_{lat} = [-1,\ \ -2,\ \ -1.5 + 0.5i,\ \ -1.5 - 0.5i,\ \ -2.5,\ \ -3]$. The observer pole are set at

$$P_{longob} = [-10,\ \ -3,\ \ -1 + i,\ \ -1 - i,\ \ -2,\ \ -2.5]$$

It can be verified that the Eqs. (3.4) and (3.13) are satisfied. Set $P = I_{5\times5}$, then

$$D = \begin{bmatrix} 0 & -0.8400 & -0.0180 & 0 & 0 & 0 \\ -2.0380 & 0.2900 & -0.3300 & 0.0571 & 2.0380 & 0 \end{bmatrix},$$

For Case I and II, the observers can be designed similar to Section 3.3.1.

In the simulation, $x(0) = [-0.0014,\ 0.0508,\ 0.4609,\ -0.0295,\ 3.4002,\ 15.4198]^T$ while other initial values are set to zero, and $\rho = 2$. From the Figs. 3.5-3.8, the faulty residual $r_i(t)$ goes to zero while the healthy residual $r_l(t)$ does not. Therefore, the faulty actuators can be isolated. This agrees with the result from the sufficient condition.

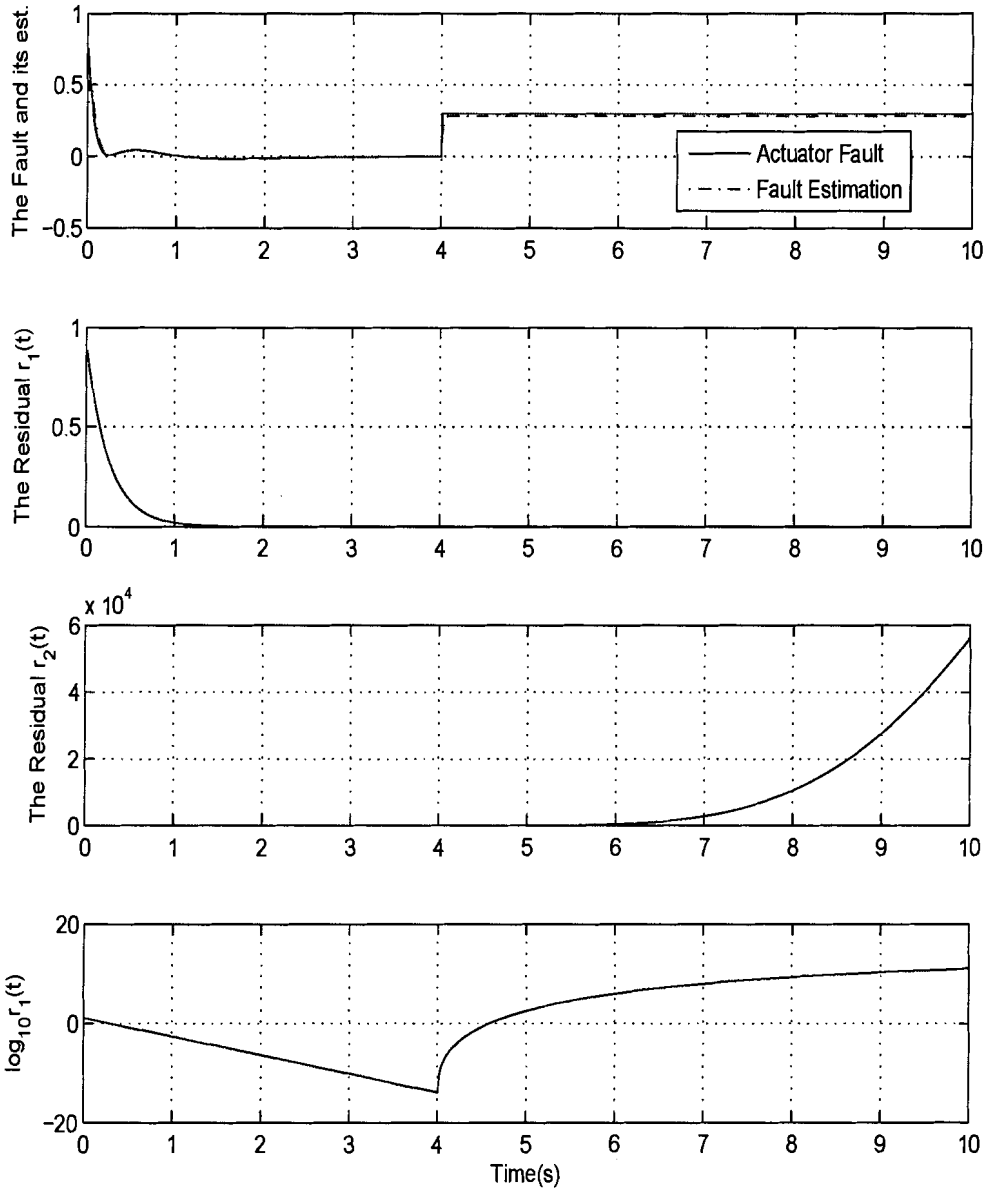


Figure 3.5: Actuator 1's fault estimation with full state measurable - Lateral Model

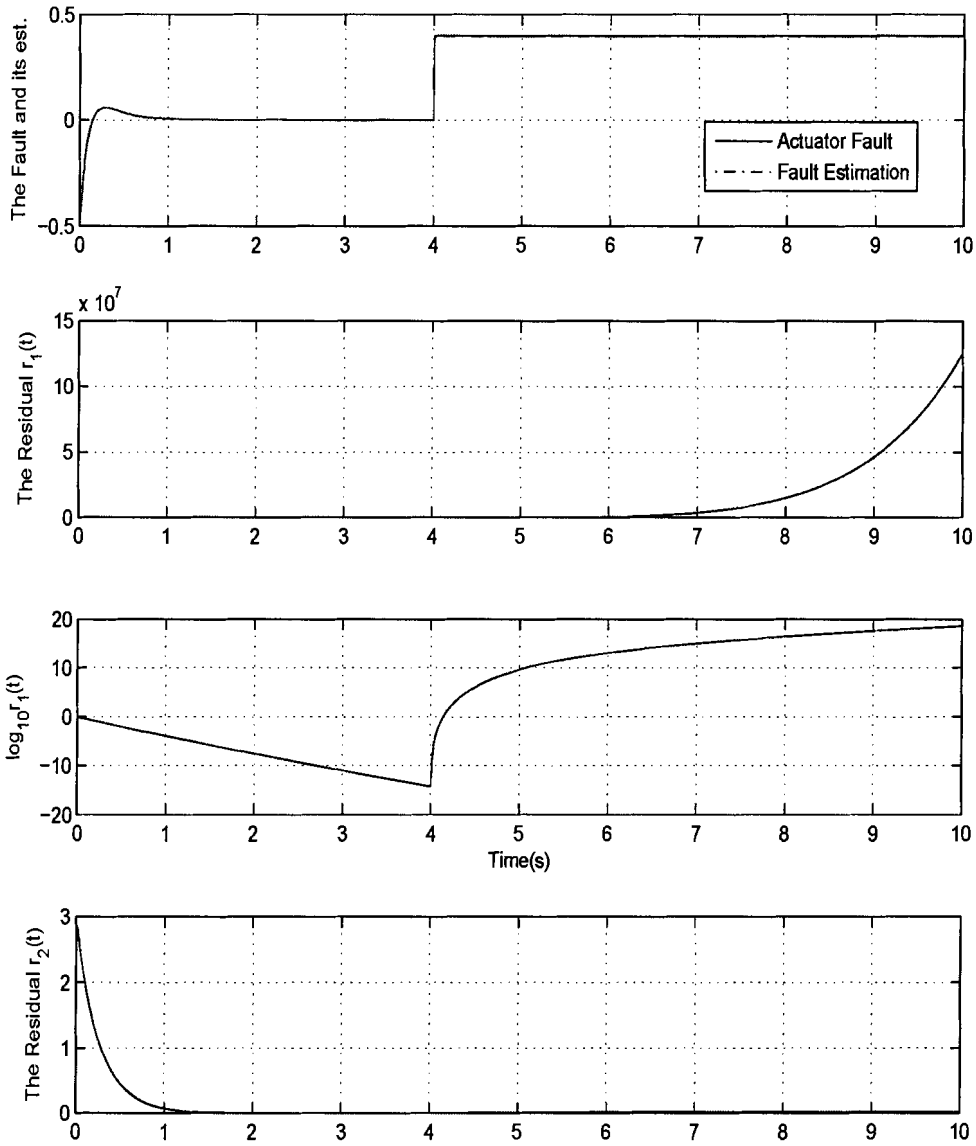


Figure 3.6: Actuator 2's fault estimation with full state measurable - Lateral Model

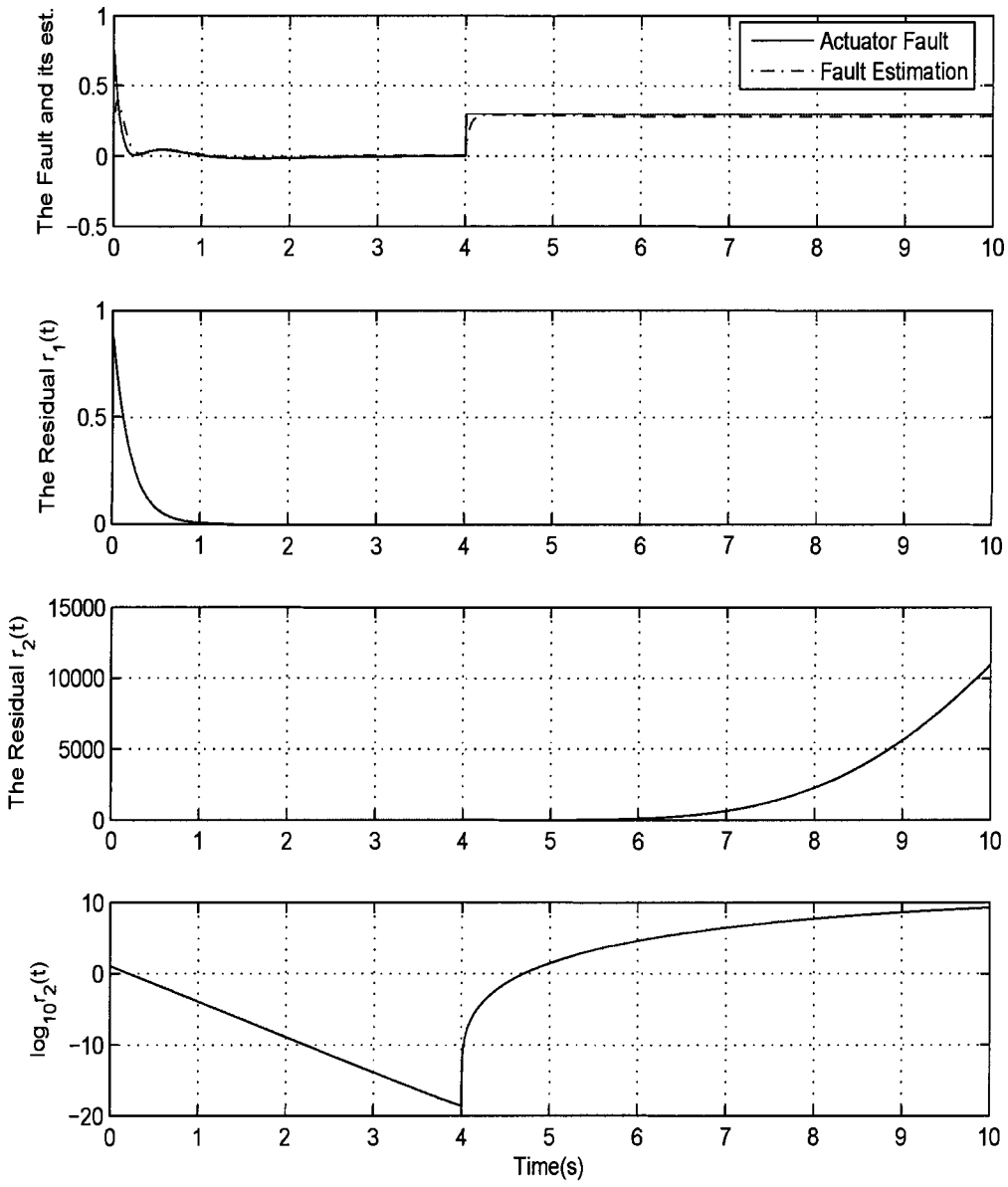


Figure 3.7: Actuator 1's fault estimation with only output measurable - Lateral Model

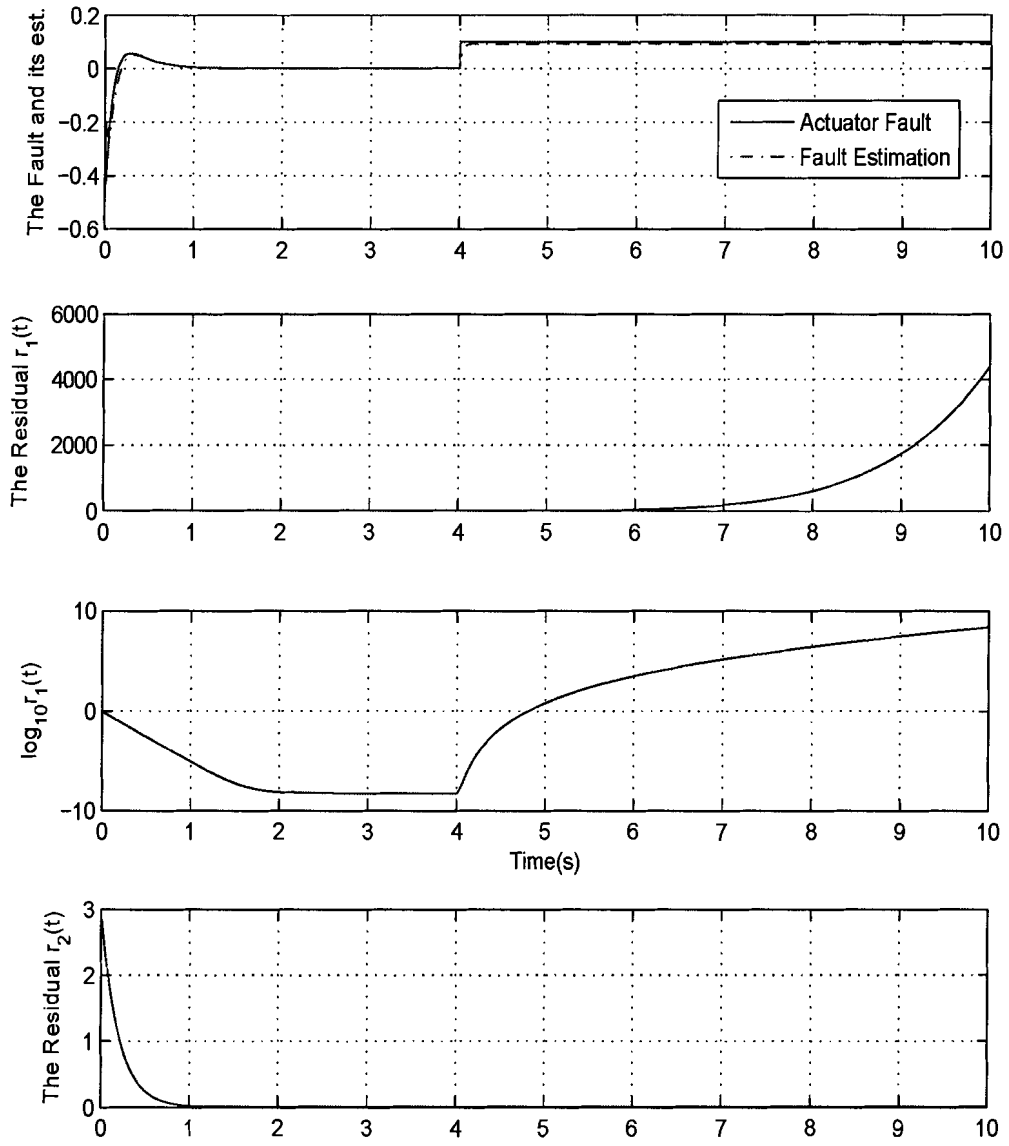


Figure 3.8: Actuator 2's fault estimation with only output measurable - Lateral Model

# Chapter 4

# Sliding Mode Observer for Actuator FDI

In the late 60s, the effect of discontinuous control action on dynamical systems was explored. At that time, the concept of sliding mode appeared in the U.S.S.R. Using an appropriate control laws, it was found that "the system states can reach and subsequently remain on a predefined surface in state space" [40]. When constrained to this surface, the inherent motion (*Sliding Motion*) is insensitive to any external disturbance or system uncertainty. Subsequently, this concept was utilized for state estimation by an observer. In this Chapter, the actuator fault isolation problem for a class of linear systems is investigated. To isolate actuator faults, we develop a fault model, then for each fault model, a Sliding Mode Observer (SMO) is designed. For the fault model corresponding to faulty actuators, the SMO can ensure that related state estimation error and thus the output estimation error can be made to go to zero. It is also shown that, for all other possible fault models, none of SMOs can make the related output estimation errors to be zero. We define the residual as the square of the magnitude of the output estimation error resulting from all possible fault models.

If one residual goes to zero, then it corresponds to faulty actuators, and actuator fault isolation is obtained. The use of the SMO has the following two advantages: It can deal with any type of bounded actuator faults (constant and non-constant faults); and it can provide a method to estimate the faults. The actuator fault isolation method was tested on a Research Civil Aircraft Model (RCAM), for which simulation results show that it effectively isolates various types of actuator faults. Portions of this chapter have been published in reference [60].

## 4.1 Introduction

When actuator faults are considered in a dynamic system, fault-tolerant control can be obtained by reconfiguring the controller to accommodate the actuator faults [30, 45, 46, 49, 51]. However, the results reported in the preceding references do not treat fault diagnosis.

Zhang, et al. [48] proposed a robust isolation scheme which can be used for actuator-fault isolation. To use the scheme, all states must be available and the unknown parameters, are also assumed to be available. Other references [44] and [47] proposed a method for the fault diagnosis that can be modeled by the product of an constant unknown parameters matrix and the system input. Excitation signals may be required to obtain accurate parameter estimation.

In Chen and Saif [56], based on a generalized observer, a bank of adaptive observers were used to isolate the actuator faults for both linear and nonlinear systems. Sufficient conditions were derived to ensure actuator-fault isolation. Due to the limitations of the adaptation technique, only constant faults were considered.

In this chapter, actuator-fault isolation for a class of linear systems with non-constant actuator faults is investigated. The faults are estimated while isolating the

faults. For this purpose, Sliding Mode Observers (SMO) are designed. Sufficient conditions for actuator-fault isolation are obtained as well.

The rest of this chapter is organized as follows. Section 2 formulates the fault isolation problem for a class of linear systems. Fault models are defined in Section 3 and we design SMOs for which some properties are proved. A sufficient condition for actuator fault isolation is derived. In Section 4, the actuator fault isolation method is applied to a Research Civil Aircraft Model (RCAM). Simulation results are presented for isolating various types of actuator faults.

## 4.2 System Description and Problem Formulation

In this section, a linear model is described and the problem of actuator-fault isolation is formulated. Additionally, assumptions are made for the SMO design and fault isolation.

Consider the following linear system

$$\begin{aligned} \dot{x} &= Ax + Bu \\ y &= Cx \end{aligned} \tag{4.1}$$

where $x \in R^n$ is the state vector, $y \in R^p$ is the output vector, and $u \in R^m$ is the input vector (the output of actuators). Matrix $B$ is called the distribution matrix of the actuators.

It is assumed that only actuator faults occur and no sensor faults are possible. Without loss of generality, we assume only a single actuator is faulty at a time.

The actuator fault isolation problem is formulated as follows. Using the available output $y$, design an sliding mode observer based scheme to isolate a faulty actuator after the fault has been detected, and estimate the faults.

We shall solve the problem using SMO theory. To obtain actuator fault isolation and fault estimation properties, the following assumptions are needed.

Assumption $A1$: $B$ has full column rank.

Assumption $A2$: When the $l$-th actuator is faulty and the actuator's output is $u_l^f(t)$, it is assumed that $|u_l^f(t)| \leq M$, where $M$ is a constant and $lim_{t\to\infty}|u_l(t) - u_l^f(t)| \neq 0$.

Assumption $A3$: There exist a positive definite matrix $P$ and matrices $L$ and $F$ such that

$$\begin{aligned} (A-LC)^T P + P(A-LC) &\leq 0 \\ PB &= C^T F^T \end{aligned} \tag{4.2}$$

**Remark 4.2.1** *Assumption 2 describes the type of actuator faults that can be treated. Essentially, it allows any type of bounded actuator faults (including constant faults).*

## 4.3 SMO With Actuator Fault Isolation and Estimation

In this section, a bank of SMOs is designed, and some properties of the SMOs are proved. A sufficient condition for actuator fault isolation is derived, and a method for fault estimation method is proposed.

### 4.3.1 Fault models

If an actuator is faulty, the resulting system from Eq. (4.1) is called a *fault model.* Since there are $m$ actuators and only a single fault is considered, there are $m$ possible

fault models, which are described for $1 \leq i \leq m$ as follows:

$$\begin{aligned} \dot{x} &= Ax + \sum_{j \neq i} b_j u_j + b_i u_i^f(t) \\ y &= Cx \end{aligned} \tag{4.3}$$

where $B = (b_1 | \cdots | b_m)$ and for $1 \leq j \leq m$, $u_j$ is the desired control effort when the $j$th actuator is healthy.

When all actuators are operating normally, the corresponding system is different from Eq. (4.3). When the $l$th actuator is faulty, then the system reduces to the $l$th fault model, which is different from any other fault models.

Fault detection can be performed by using the observer

$$\dot{\hat{x}} = A\hat{x} - L(C\hat{x} - y) + Bu \tag{4.4}$$

where $L$ is chosen so that $A - LC$ is a Hurwitz matrix.
Based on Eq. (4.4), a residual for fault detection is defined as $r_i(t) = |C\hat{x}_i - y_i|^2$, where $1 \leq i \leq m$. If one residual goes to zero with all others does not converge to zero, then the faulty actuator can be identified as the one corresponding to its residual approaching zero.

### 4.3.2 SMO for Fault Models and their Properties

In the last subsection, we defined $m$ possible fault models. If the $l$th actuator is faulty, the Eq. (4.1) reduces to the $l$th fault model as follows:

$$\begin{aligned} \dot{x} &= Ax + \sum_{j \neq l} b_j u_j + b_l u_l^f(t) \\ y &= Cx \end{aligned} \tag{4.5}$$

The measured output is that of the above fault model.

By using the SMO design technique, we can design a bank of observers for all possible fault models as follows:

$$\begin{aligned} \dot{\hat{x}}_i &= A\hat{x}_i - L(\hat{y}_i - y) + \sum_{j \neq i} b_j u_j + b_i \mu_i \\ \mu_i &= -\rho \frac{F_i e_{y_i}}{|F_i e_{y_i}|}, \ 1 \leq i \leq m \end{aligned} \tag{4.6}$$

where $F_i$ is the $i$th row of $F$, $\rho$ is chosen such that $\rho \geq M$, and $e_{y_i}$ is defined as $e_{y_i} = C\hat{x}_i - y = Ce_{x_i}$.

In Eq. (4.6), the matrix equation and inequality have to be solved for $P$, $L$ and $F$ in Eq. (4.2). It can be shown that finding $P$, $L$ and $F$ in Eq. (4.2) is equivalent to solve the following LMIs for $P$, $Y$ and $F$.

$$\begin{aligned} \begin{pmatrix} A^TP + PA + C^TY^T + YC & PB - C^TF^T \\ B^TP - FC & 0 \end{pmatrix} &\leq 0 \\ A^TP + PA + C^TY^T + YC &\leq 0 \end{aligned} \tag{4.7}$$

where $L = -P^{-1}Y$. From here the solutions can be found using standard LMI algorithms [61].

The designed SMO has the following properties.

**Theorem 4.1** *With assumptions A1 $\sim$ A3, if the lth actuator is faulty, then for $i = l$,*

$$lim_{t \to \infty} e_{x_l} = 0 \tag{4.8}$$

*and for $i \neq l$,*

$$lim_{t \to \infty} e_{x_l} \neq 0 \tag{4.9}$$

Proof: For $i = l$, $H = A - LC$. It follows from Eqs. (4.5) and (4.6) that

$$\dot{e_{x_l}} = He_{x_l} + b_l(\mu_l(t) - u_l^f) \tag{4.10}$$

Choose a Lyapunov function

$$V = (e_{x_l})^T P e_{x_l} \tag{4.11}$$

And define $Q = -(A - LC)^T P - P(A - LC)$. Differentiating the Lyapunov function with respect to the time, and using Eq. (4.10) and the Eq. (4.6),derived that

$$\begin{aligned}
\dot{V} &= -(e_{x_l})^T Q e_{x_l} + 2(e_{x_l})^T P b_l(\mu_l(t) - u_l^f) \\
&= -(e_{x_l})^T Q e_{x_l} + 2(F_l C e_{x_l})^T(\mu_l(t) - u_l^f) \\
&= -(e_{x_l})^T Q e_{x_l} + 2(F_l e_{y_l})^T(\mu_l(t) - u_l^f) \\
&\leq -(e_{x_l})^T Q e_{x_l} - 2|F_l e_{y_l}|(\rho - M) \\
&\leq -(e_{x_l})^T Q e_{x_l}
\end{aligned} \tag{4.12}$$

Because $P$ and $Q$ are positive definite, $|e_{x_l}|$ tends to zero exponentially. The first part of the theorem have been proved.

For $i \neq l$, it follows from Eqs. (4.5) and (4.6) that

$$\dot{e}_{x_i} = He_{x_i} + b_i(\mu_i - u_i) + b_l(u_l(t) - u_l^f) \tag{4.13}$$

Because $lim_{t\to\infty}|u_l(t)| - |u_l^f(t)| \neq 0$, and $b_i$ and $b_l$ are independent (assumption $A3$),

$$lim_{t\to\infty}[b_i(\mu_i - u_i) + b_l(u_l(t) - u_l^f)] \neq 0$$

Together with Eq. (4.13), this implies that $lim_{t\to\infty}e_{x_i} \neq 0$. And the proof is complete. ¶

### 4.3.3 Actuator Fault Isolation and Estimation

If the residuals are defined as $r_i(t) = \|e_{y_i}(t)\|^2$ for $1 \leq i \leq m$, then, based on Theorem 4.1, a sufficient condition for actuator fault isolation is obtained as follows.

**Theorem 4.2** *With assumptions A1 $\sim$ A3, if any two columns of CB are independent, then fault actuator isolation can be obtained by evaluating the residuals resulting from Eq. (4.6).*

Proof: Based on Theorem 4.1, if the $l$th actuator is faulty, $r_l(t) = \|e_{y_l}(t)\|^2 = \|Ce_{x_l}\|^2$ tends to zero.

Because $C$ in nonsingular, from Theorem 4.1 and for any $i \neq l$, the residual $r_i(t) = \|e_{y_i}(t)\|^2 = \|Ce_{x_i}\|^2$ does not always go to zero as on any small time intervals. Except for some very special cases, we would have that $r_i(t)$ does not tend to zero for any $i$ *neql*. Because the residual corresponding to a faulty actuator goes to zero while the others do not, the faulty actuator can be isolated successfully by monitoring $r_i(t)$. This completes the proof. ¶

The above theorem guarantees that a bank of SMOs can be used for actuator fault isolation. The only difficulty is the realization of the SMOs because of chattering. To reduce chattering, a modified SMO is proposed as follows:

$$\begin{aligned} \dot{\hat{x}}_i &= A\hat{x}_i - L(\hat{y}_i - y) + \sum_{j \neq i} b_j u_j + b_i \mu_i \\ \mu_i &= -\rho \frac{F_i e_{y_i}}{|F_i e_{y_i}| + \delta}, \ 1 \leq i \leq m \end{aligned} \tag{4.14}$$

where $\delta$ is very small constant.

For the fault model corresponding to a faulty actuator, and according to Theorem 4.1, $r_l(t) = \|e_{y_l}(t)\|^2$ should be small if $\delta$ is small, while other residuals $r_i(t) = \|e_{y_i}(t)\|^2$

for $i \neq l$ are larger. Therefore, by choosing a suitable threshold, actuator faults can be isolated using a bank of modified SMOs.

Once the $l$th actuator is identified as faulty, $\|e_{x_l}\|$ must be small. If we assume that $\|\dot{e_{x_l}}\|$ is also small, and based on (4.10), a method to estimate the actuator fault is as follows.

$$\hat{u}_l^f = \mu_l(t) = -\rho \frac{F_l e_{y_l}}{|F_l e_{y_l}| + \delta} \tag{4.15}$$

where $\hat{u}_l^f$ is the estimation of the actuator fault $u_l^f$.

## 4.4 Actuator Fault Isolation on a Research Civil Aircraft Model

### 4.4.1 Research Civil Aircraft Model

The Research Civil Aircraft has been discussed in Chapter 2. For convenience, the models are repeated as follows:

- Longitudinal:

$$A_{long} = \begin{bmatrix} -0.98 & 0 & 0 & -0.016 & 0 \\ 1.00 & 0 & 0 & 0 & 0 \\ -2.190 & -9.780 & -0.028 & 0.074 & 0 \\ 77.360 & -0.770 & -0.220 & -0.670 & 0 \\ 0 & -79.97 & -0.03 & 0.99 & 0 \end{bmatrix}, \quad B_{long} = \begin{bmatrix} -2.44 & 0.58 \\ 0 & 0 \\ 0.180 & 19.620 \\ -6.480 & 0 \\ 0 & 0 \end{bmatrix},$$

$$C_{long} = \begin{bmatrix} 1 & 0 & 0 & 0 & 0 \\ 7.88 & -0.078 & -0.023 & -0.068 & 0 \\ 0 & 0 & 0.99 & 0.029 & 0 \\ 0 & -79.97 & -0.028 & 0.99 & 0 \\ 0 & 0 & 0 & 0 & 1 \end{bmatrix}$$

with

$$\begin{aligned} x_{long} &= [q\ \theta\ u_B\ w_B\ z]^T \\ y_{long} &= [q\ n_Z\ V_A\ w_E\ z]^T \\ u_{long} &= [\delta_t\ \delta_{th}]^T \end{aligned} \tag{4.16}$$

The longitudinal control objective is to design a feedback controller to make the state vector $x$ stay at

$$b = [0,\quad 0.0678,\quad 79.98,\quad 0.861,\quad 305]^T$$

To realize the above control goal, we utilize the following feedback controller:

$$\begin{aligned} x &= C^{-1}y \\ u &= -K(x-b)+u_c \end{aligned} \tag{4.17}$$

where $K$ is chosen such that the closed-loop poles are assigned at $K_{long} = [-1,\quad -2,\quad -0.5,\quad -0.3,\quad -1.5]$, and $u_c = [0.1865,\quad 0.009]^T$ is a solution of $Ab + Bu = 0$.

If there are no faults, this controller can indeed drive the system state vector asymptotically to $b$. Denote $B = [B1\ \ B2]$, $K = \begin{bmatrix} K1 \\ K2 \end{bmatrix}$, it can be verified that both $A - B1K1$ and $A - B2K2$ are Hurwitz matrices. This is necessary for the case that actuator faults occur.

- Lateral:

$$A_{lat} = \begin{bmatrix} -1.270 & 0.550 & 0 & 0 & -0.024 & 0 \\ 0.052 & -0.502 & 0 & 0 & 0.005 & 0 \\ 1.000 & 0.028 & 0 & 0 & 0 & 0 \\ 0 & 1.000 & 0 & 0 & 0 & 0 \\ 2.270 & -79.00 & 9.970 & 0 & -0.170 & 0 \\ 0 & 0 & 0 & 0 & 0 & 1 \end{bmatrix},\quad B_{lat} = \begin{bmatrix} -0.840 & 0.290 \\ -0.018 & -0.330 \\ 0 & 0 \\ 0 & 2.038 \\ 0 & 0 \\ 0 & 0 \end{bmatrix},$$

$$C_{lat} = \begin{bmatrix} 0 & 0 & 0 & 0 & 0.013 \\ 1.000 & 0 & 0 & 0 & 0 \\ 0 & 1.000 & 0 & 0 & 0 \\ 0 & 0 & 1.000 & 0 & 0 \\ 0 & 0 & -0.028 & 1.000 & 0.013 \\ 0 & 0 & -2.260 & 79.87 & 1.000 \end{bmatrix}$$

with

$$\begin{aligned} x_{lat} &= [p \ r \ \phi \ \psi \ v_B \ y_p]^T \\ u_{lat} &= [\delta_a \ \delta_r]^T \\ y_{lat} &= [\beta \ p \ r \ \phi \ \chi \ y_p]^T \end{aligned} \tag{4.18}$$

In similar cases, the lateral feedback gain can be chosen to place closed loop poles at

$$K_{lat} = [-1, \ -2, \ -1.5 + 0.5i, \ -1.5 - 0.5i, \ -2.5, \ -3]$$

.

The observer poles are set at

$$P_{longob} = [-10, \ -3, \ -1 + i, \ -1 - i, \ -2, \ -2.5]$$

### 4.4.2 SMOs design for the actuator fault isolation and estimation

There are two possible fault models for two actuators. Based on these fault models and Section 3, two SMOs are obtained as follows:

$$\begin{aligned} \dot{\hat{x}}_1 &= A\hat{x}_1 - L(\hat{y}_1 - y) + b_2 u_2 + b_1 \mu_1 \\ \mu_1 &= -\rho \frac{(e_{y_1})^T (C^{-1})^T P b_1}{|(e_{y_1})^T (C^{-1})^T P b_1|} \end{aligned} \tag{4.19}$$

and

$$\begin{aligned} \dot{\hat{x}}_2 &= A\hat{x}_2 - L(\hat{y}_2 - y) + b_1 u_1 + b_2 \mu_2 \\ \mu_2 &= -\rho \frac{(e_{y_2})^T (C^{-1})^T P b_2}{|(e_{y_2})^T (C^{-1})^T P b_2|} \end{aligned} \tag{4.20}$$

where $L = (A-H)C^{-1}$, $P$ and $Q$ are positive definite matrices such that $H^T P + PH = -Q$, $\rho$ is chosen such that $\rho \geq F$, and $e_{y_i} = C\hat{x}_i - y = Ce_{x_i}$.

If the first actuator is faulty, the fault can be estimated by $\mu_1$. Otherwise, it can be estimated by $\mu_2$.

### 4.4.3 Simulation Results

For the longitudinal model, we let $H = -2I_{5\times5}$, $Q = 4I_{5\times5}$, and hence $P = I$. In all simulations, the feedback controller described in Chapter 3 was applied. It is assumed that the state vector is very close to $b$ at $t = 0$ and the first actuator has been faulty since $t = 1s$. Thus, the initial conditions are chosen as $x(0) = b$ and $x_1^T(0) = x_2^T(0) = [\,b_1, \quad 0.999b_2, \quad b_3, \quad 0.999b_4, \quad b_5\,]$.

For the lateral model, we let $H = -2I_{6\times6}$, $Q = 4I_{6\times6}$, and hence $P = I$. The lateral control objective is to design a feedback controller to make the state vector $x$ stay at the neutral position which is $b = [0,\ 0,\ 0,\ 0,\ 0,\ 0,]^T$. The feedback gain was chosen as $K_{lat} = [-1, \quad -2, \quad -1.5 + 0.5i, \quad -1.5 - 0.5i, \quad -2.5, \quad -3]$. The observer poles were set at

$$P_{longob} = [-10, \quad -3, \quad -1 + i, \quad -1 - i, \quad -2, \quad -2.5]$$

In the simulations, $x(0) = [-0.0014, \quad 0.0508, \quad 0.4609, \quad -0.0295, \quad 3.4002, \quad 15.4198]^T$ and other initial values are set to zero.

Three kinds of faults are considered. The first one is constant, i.e., $u_1^f = 0.4$. The second one is an incipient fault which is assigned as $u_1^f = e^{-0.05t}u_1(t) + \frac{t}{4t+10}$. The last

one is due to the loss of effectiveness, i.e. $u_1^f = 0.5u_1(t)$. The corresponding simulation results for RCAM longitudinal and lateral models are plotted in Figure 4.1 to Figure 4.12. In Figures 4.1, 4.3, 4.5 and 4.7, 4.9, 4.11 the residuals corresponding to the first actuator and the estimation of the fault are depicted. In Figures 4.2, 4.4, 4.6 and 4.8, 4.10, 4.12, the residuals corresponding to the second actuator are plotted. In the remaining figures, the healthy actuator estimation is plotted twice. One plot has a normal scale, the other is a logarithmic scale. From each of figures, we see that one residual approaches zero as $t$ increases. However, the other residual remains nonzero as $t$ increases. This observation shows that all three faults can be isolated successfully. The three actuator faults are estimated accurately within one or two seconds.

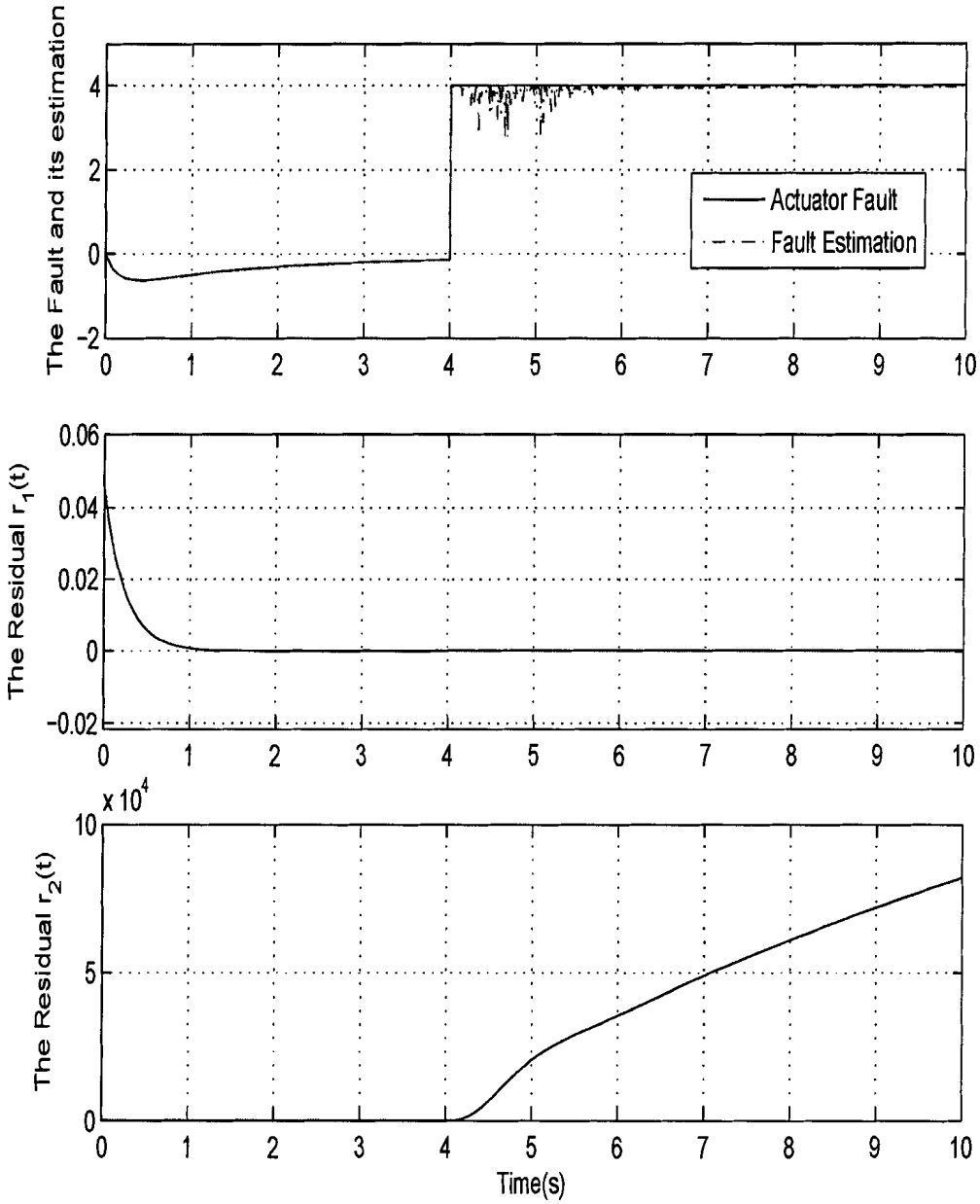


Figure 4.1: Actuator 1's fault estimation with constant fault - longitudinal model

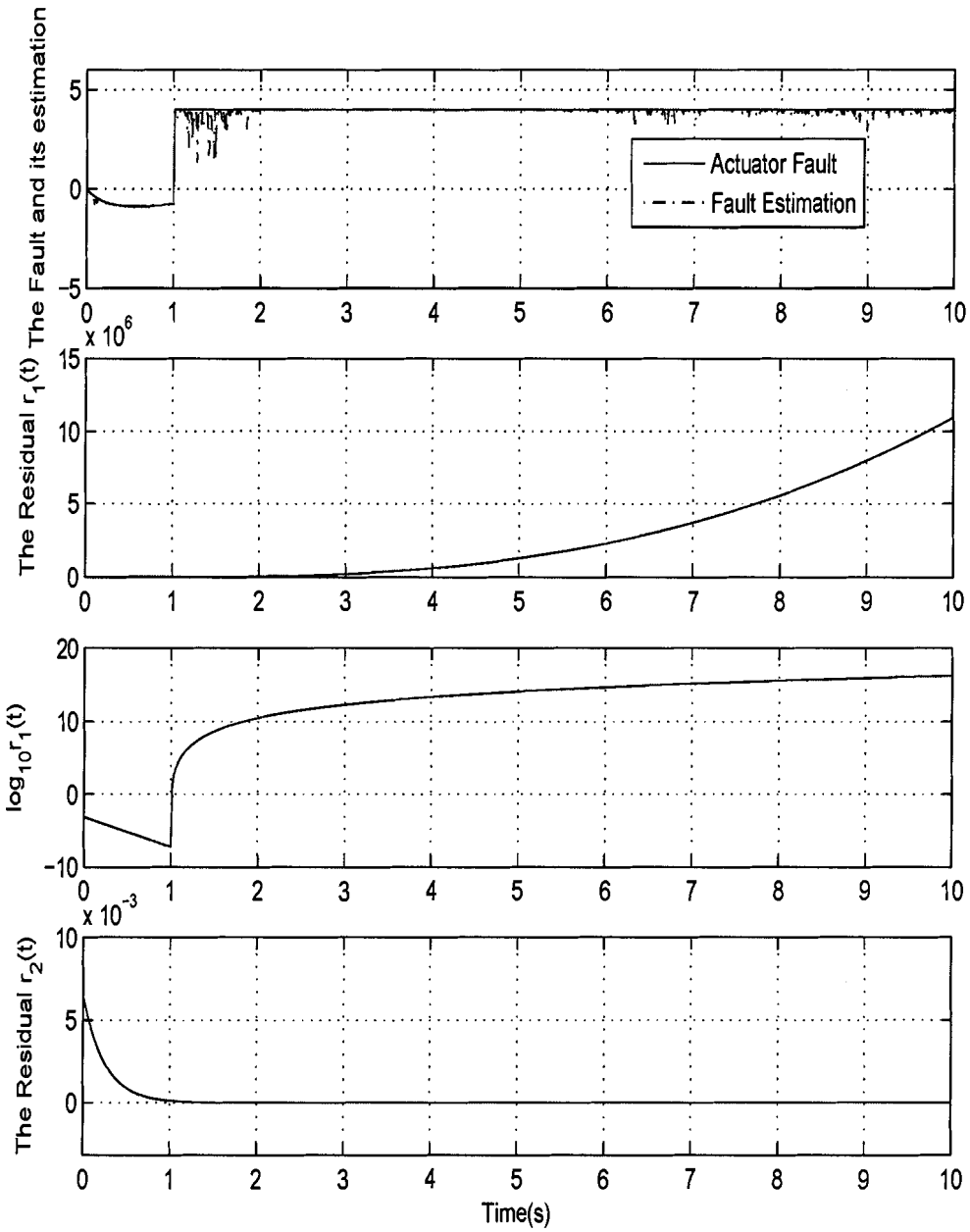


Figure 4.2: Actuator 2's fault estimation with constant fault - longitudinal model

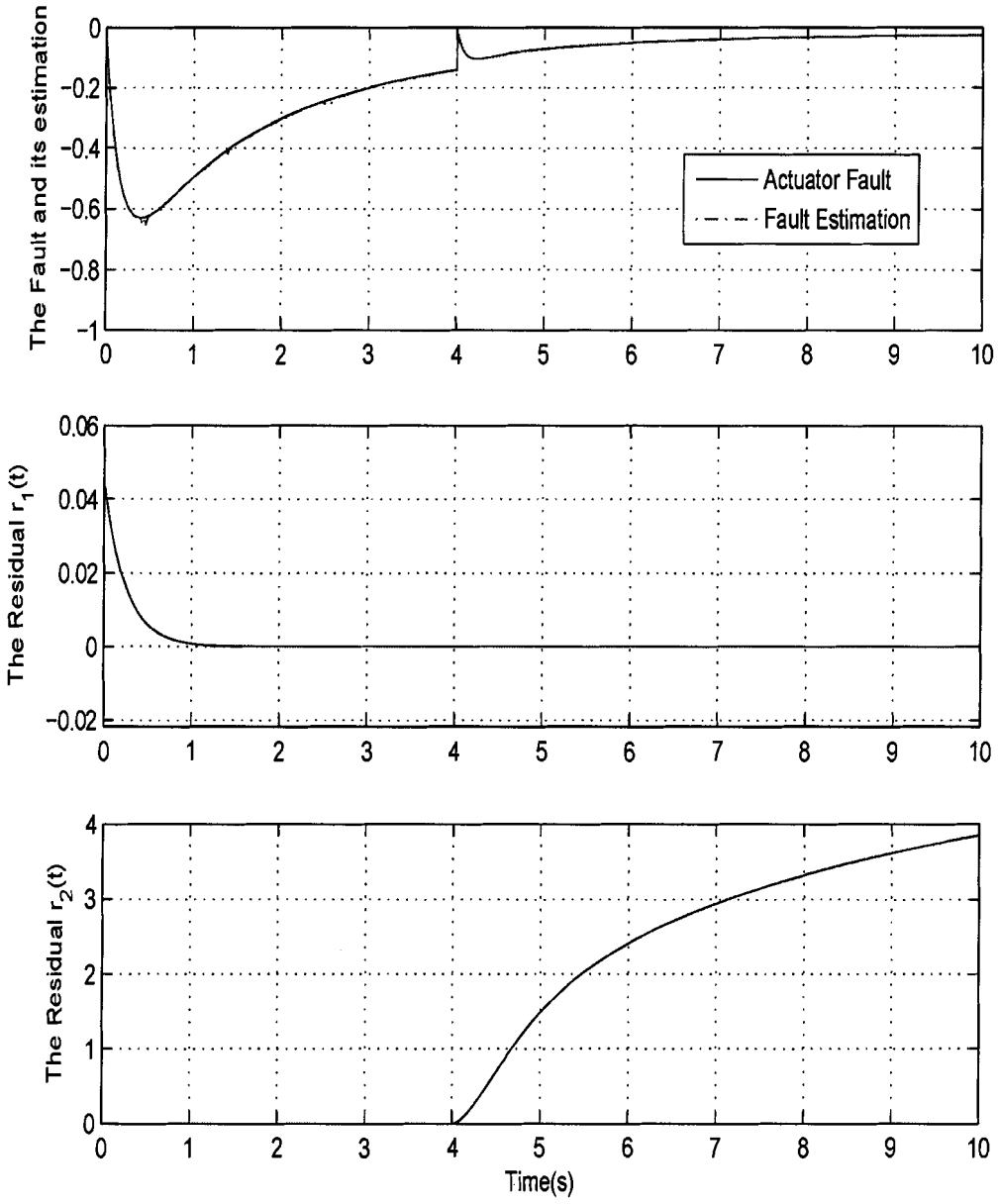


Figure 4.3: Actuator 1's fault estimation with incipient fault - longitudinal model

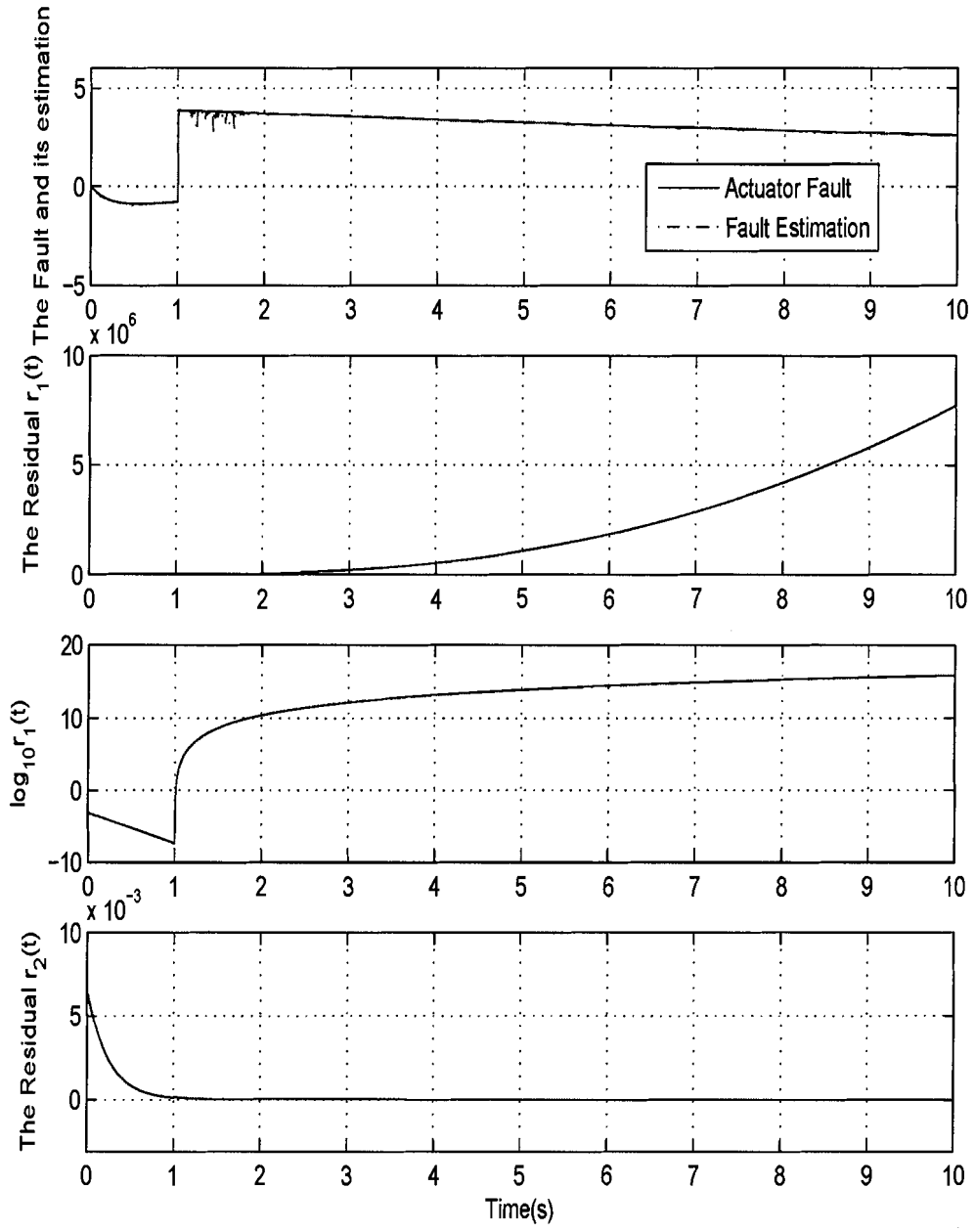


Figure 4.4: Actuator 2's fault estimation with incipient fault - longitudinal model

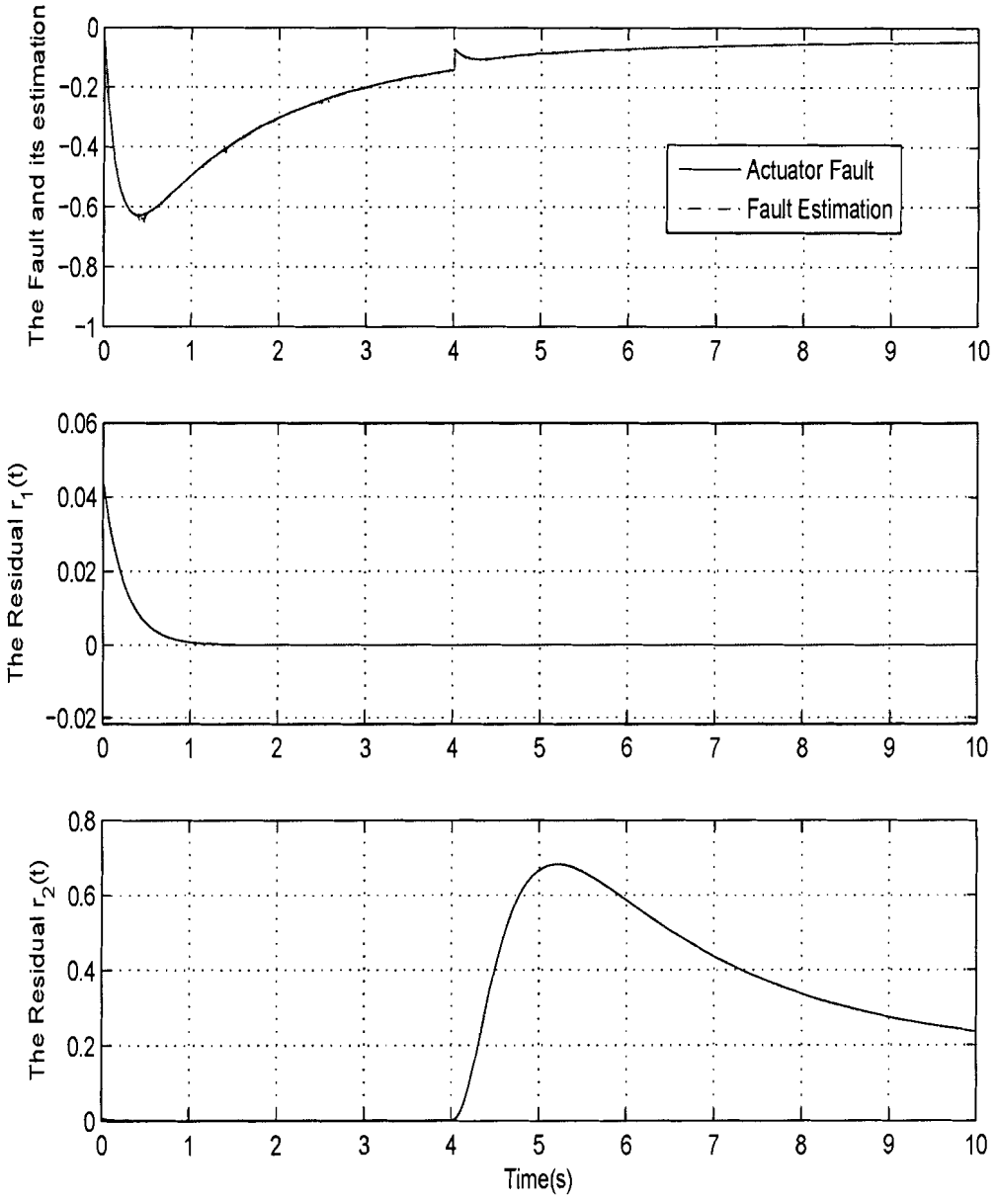


Figure 4.5: Actuator 1's fault estimation with loss-of-effectiveness fault - longitudinal model

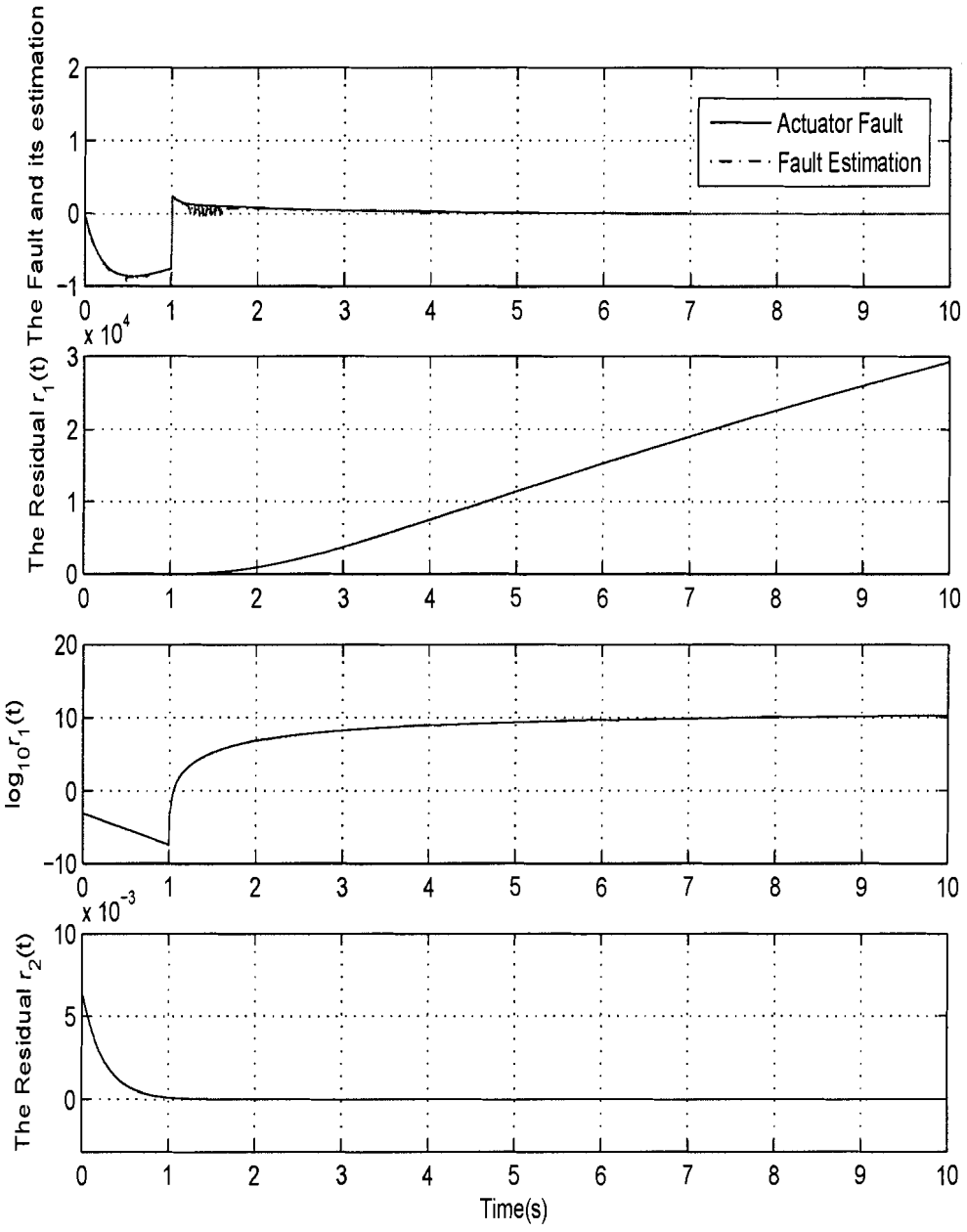


Figure 4.6: Actuator 2's fault estimation with loss-of-effectiveness fault - longitudinal model

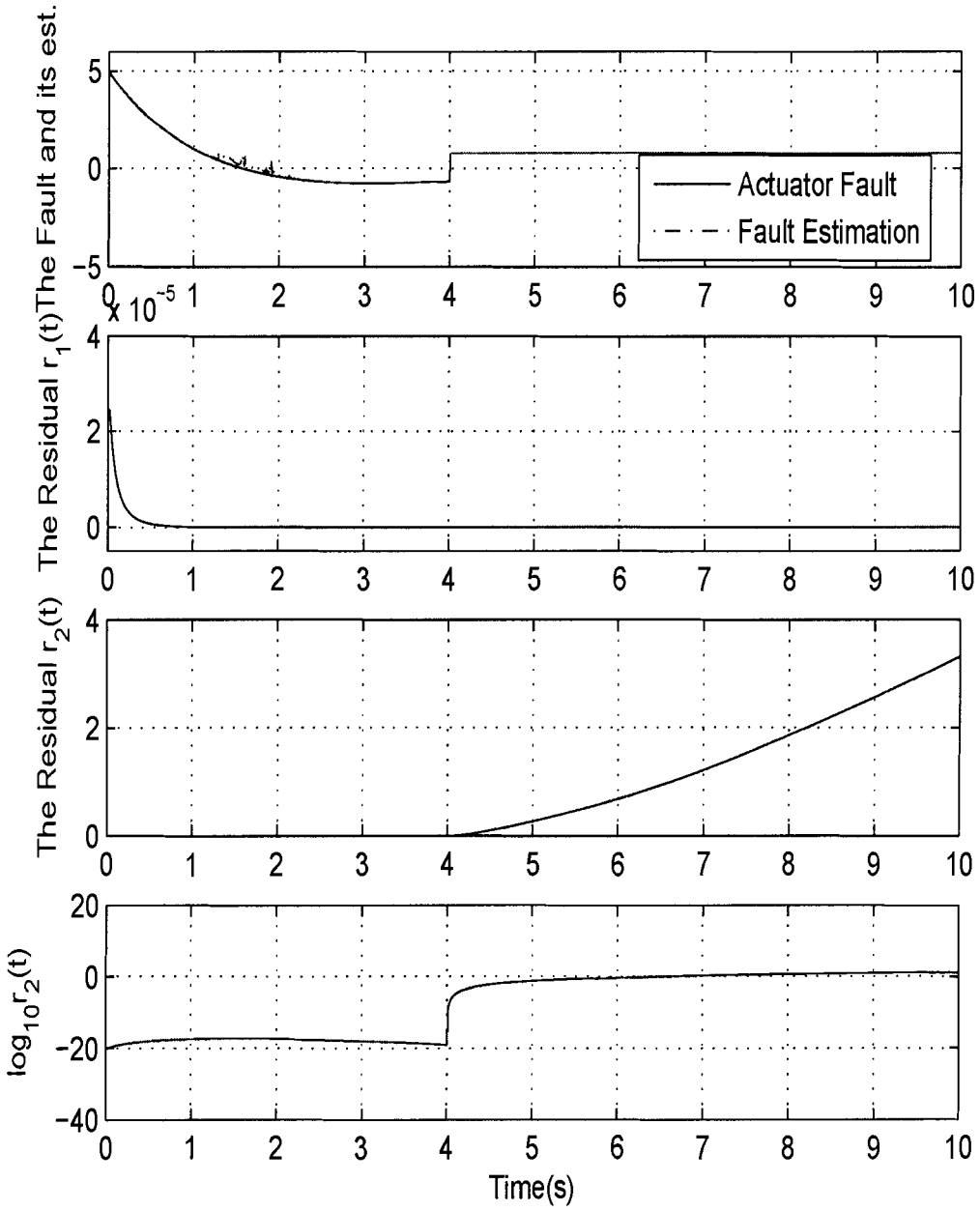


Figure 4.7: Actuator 1's fault estimation with constant fault - lateral model

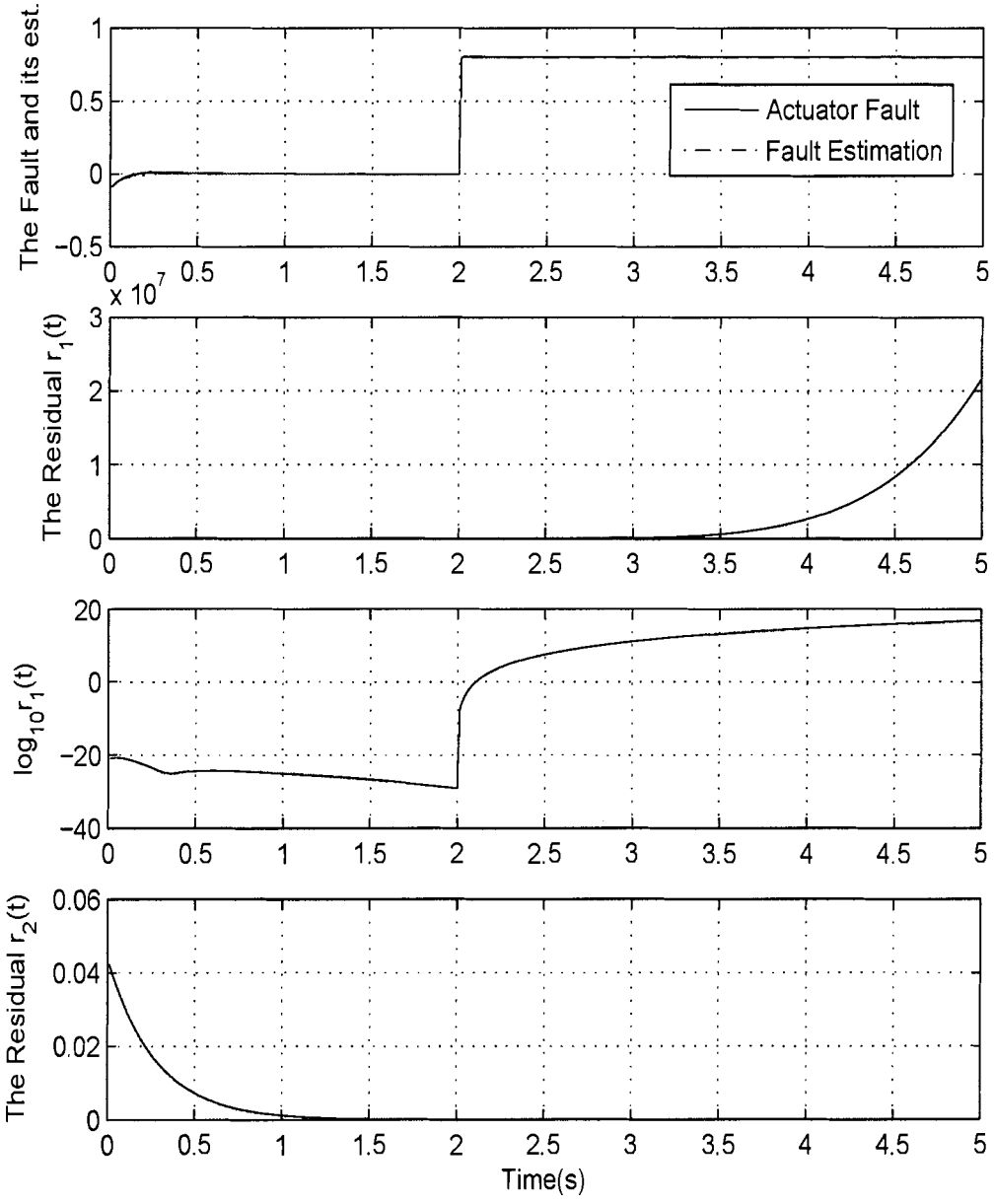


Figure 4.8: Actuator 2's fault estimation with constant fault - lateral model

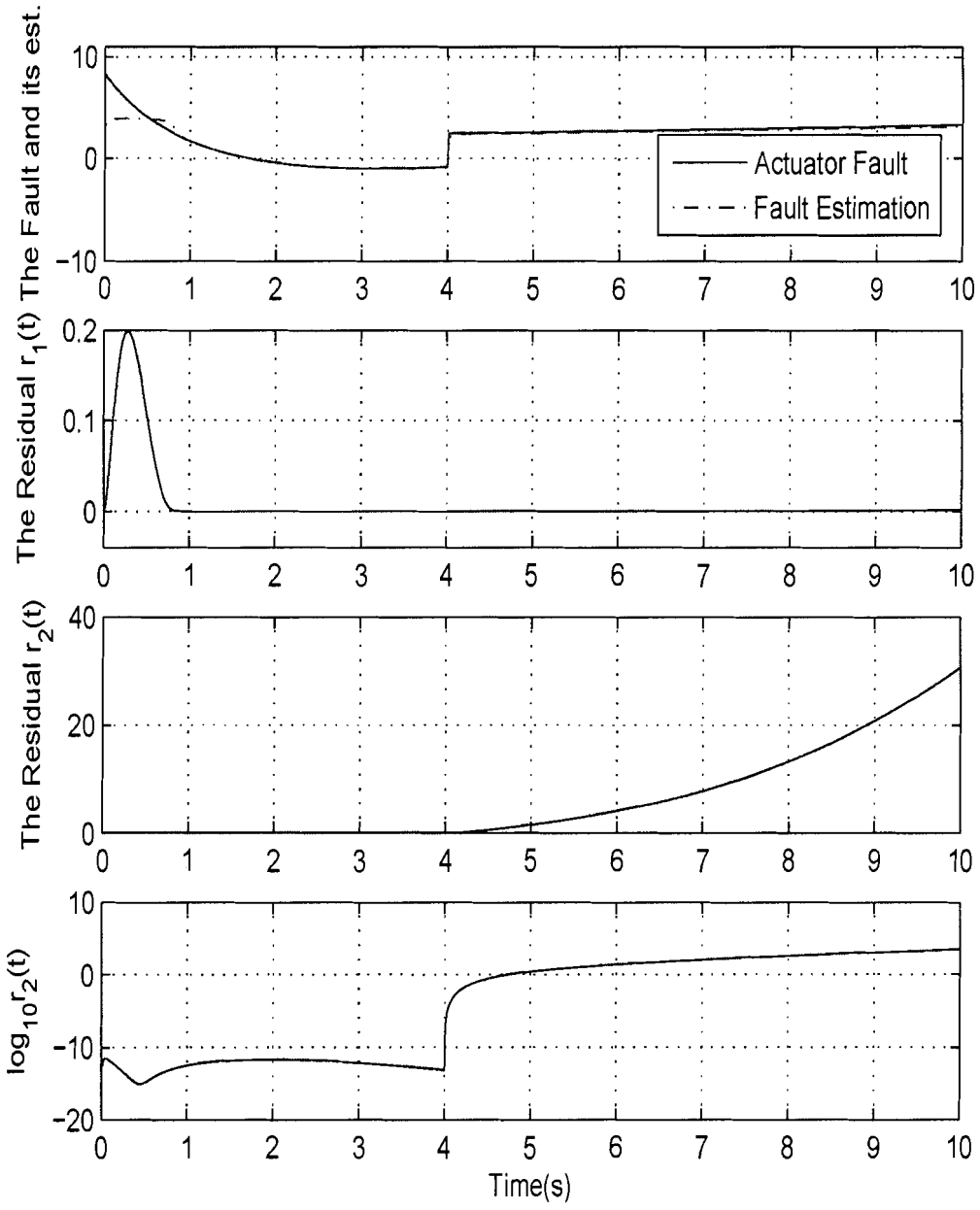


Figure 4.9: Actuator 1's fault estimation with incipient fault - lateral model

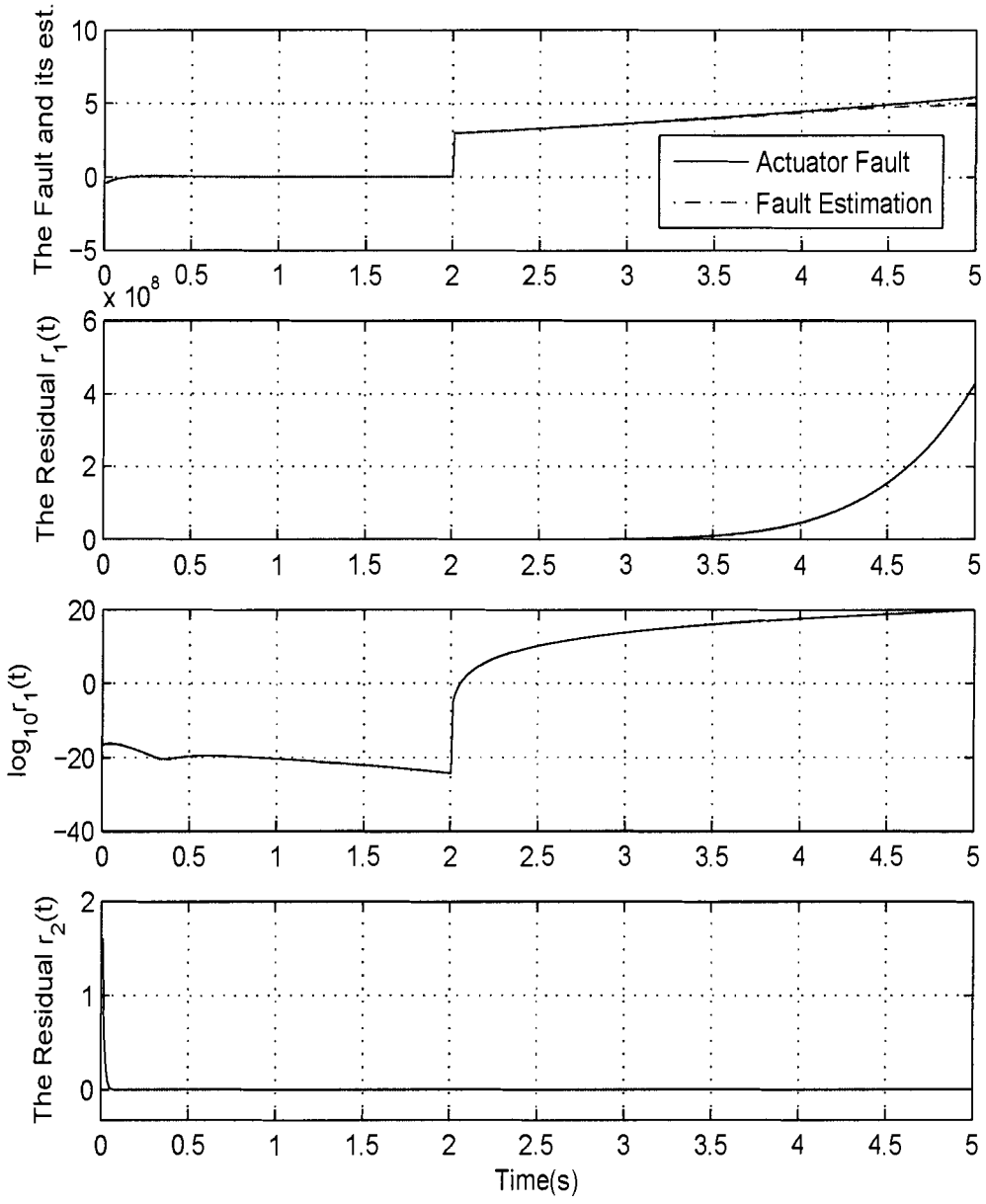


Figure 4.10: Actuator 2's fault estimation with incipient fault - lateral model

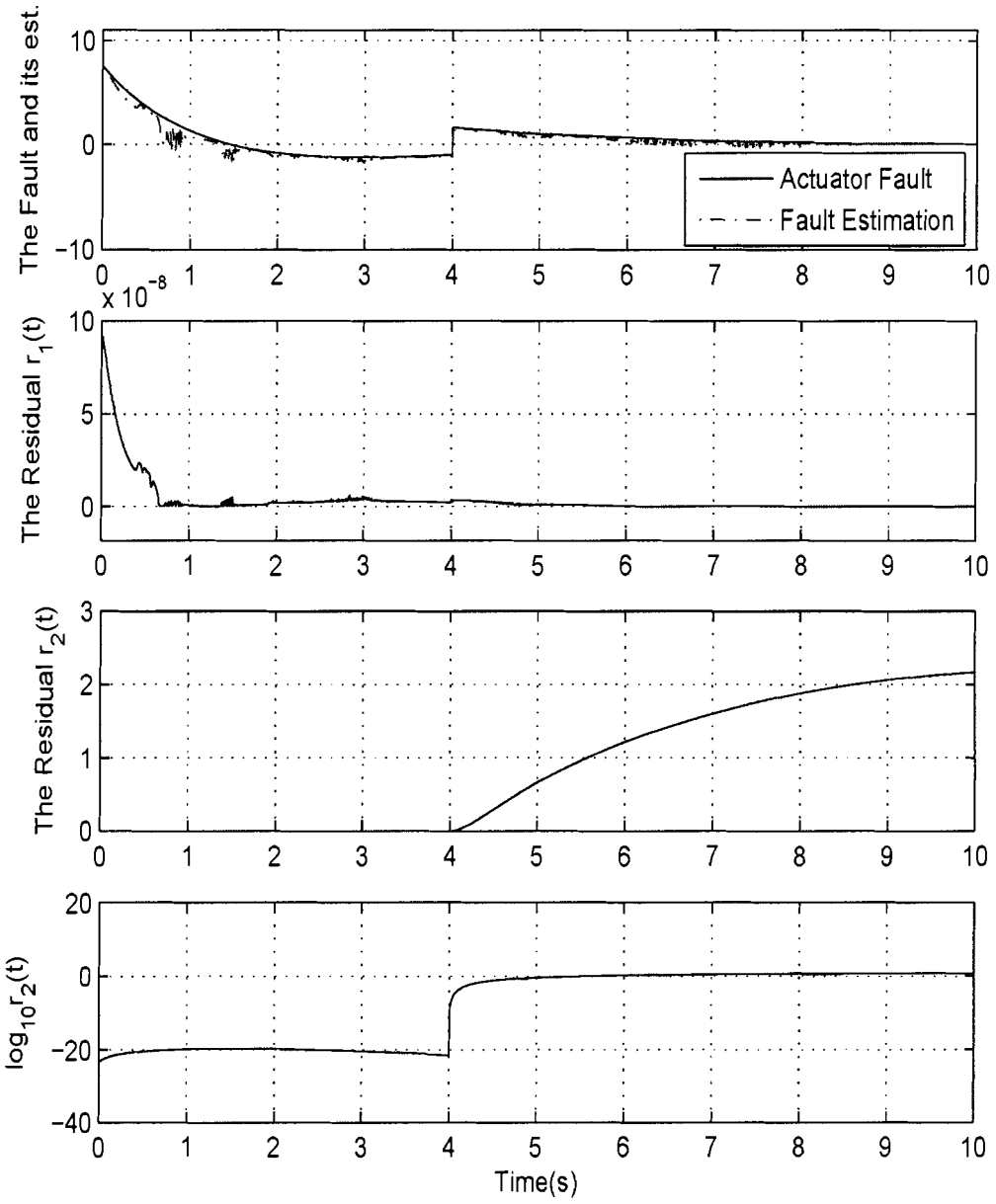


Figure 4.11: Actuator 1's fault estimation with loss-of-effectiveness fault - lateral model

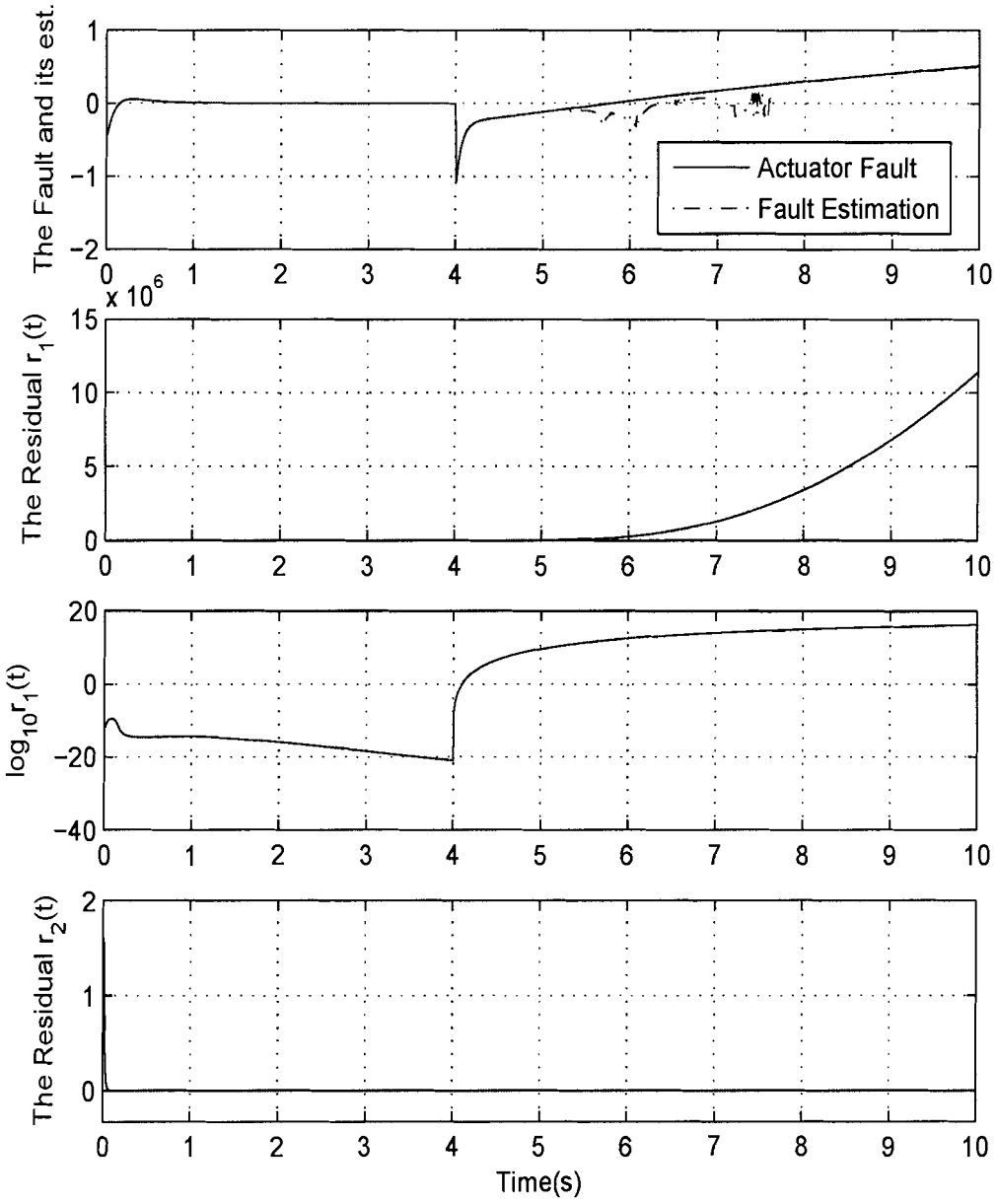


Figure 4.12: Actuator 2's fault estimation with loss-of-effectiveness fault - lateral model

# Chapter 5

# Conclusions and Further Work

## 5.1 Conclusions

Adaptive observers and sliding mode observers (SMO) based fault diagnosis schemes were designed and tested on Research Civil Aircraft Model for the purpose of fault diagnosis. The main contribution of this thesis is the design of the adaptive observers and sliding mode observers that have been used to detect, isolate and estimate the actuator faults.

The widely used methods for fault diagnosis are observer based as demonstrated in the thesis. The basic idea behind the utilization of observers for fault diagnosis is to estimate the system's states and the system's outputs from measurements by using observers. Residuals are then constructed by weighted output estimations. The residuals are then used for FDI purposes.

In Chapter 3, actuator fault isolation scheme based on adaptive observers for linear systems with measurable all states and with measurable only outputs is considered. Sufficient conditions for actuator fault isolation are derived. The adaptive observer

constructed according to the linear system can achieve both fault detection and estimation. The simulation results verify that the adaptive observer can efficiently detect and estimate actuator faults in the aircraft systems.

the adaptive observer based scheme was proved to work well for constant actuator fault detection, isolation and estimation. One disadvantage of adaptive observer based scheme is that it can only detect and isolate constant faults.

In practice, various types of faults may occur. To deal with non constant faults, sliding mode observer based schemes were proposed. This approach can detect, isolate, and estimate both constant and time-varying faults.

The SMO, proposed in Chapter 4, is a robust observer that can eliminate the effects of disturbances on the estimation error dynamics. That is, it can detect the occurrence of a fault by suppressing the disturbance.

The attractive feature of the SMO is that it can detect relatively small faults, and also supply the operation with fault estimations so that we can estimate the size and severity of the faults.

Actuator fault estimation, isolation and identification can provide valuable information to accommodate actuator faults in aircraft system and achieve the goal of maintaining the aircraft functioning.

## 5.2 Suggestions for Further Work

The main contributions of this work have been demonstrated. Furthermore, there are a few future works need to be done. Extensions of the scheme to systems with disturbances, and further to nonlinear systems are the future research topics.

**Disturbance** The working condition of the aircraft and its actuators are very challenging. The temperature varies from -70 degree Celsius to as high as several

hundreds degrees inside the engine. The temperature change could generate disturbance to the behavior of the actuator. The loading changes and gust may introduce other disturbances. To design a robust observer to estimate, isolate and identify the fault from the disturbance is a major topic that can be investigated.

**Nonlinear system FDI** In practice, many systems possesses nonlinear properties. To design the FDI system, linearized model method may not give satisfactory result due to mismatch between linear model and nonlinear behavior. Therefore, future investigations are needed to extended the application to nonlinear systems.

# Bibliography


[1] Stevens, B. L. and Lewis F. L., *Aircraft Control and Simulation, Second Edition* John Wiley & Sons, Inc., 2003.

[2] International Air Transport Association (IATA), *World Air Transport Statistics (WATS), 49th Edition*, IATA Press, 2004.

[3] International Air Transport Association (IATA), *IATA Annual Report 2005 Edition*, IATA Press, 2005.

[4] Demetriou, M. A. and Polycarpou, M.M., *Incipient fault diagnosis of dynamical systems using online approximators*, IEEE Transactions on Automatic Control, 43, pp. 1612-1617, 1998.

[5] Boeing, *Statistical Summary of Commercial Jet Airplane Accidents: Worldwide Operations 1959-1999, Airplane Safety*, Boeing Commercial Airplanes Group, Seattle, WA., June 2000.

[6] *Air Transportation in the 21st Century*, NASA FS-1998-07-38-LaRC, July, 1998.

[7] Krause, S. S., *Aircraft Safety: Accident Investigations, Analyses & Applications, Second Edition*, McGraw-Hill Professional, July 2003.

[8] Aerospace Industries Association, *AIA Five-Year R&D Plan for American Aerospace (2004 - 2008)*, AIA, 2003.

[9] Gilbert, B., *Use of Systems Analysis to Assess Progress toward Goals and Technology Impacts*, NASA Langley Research Center, November 15, 1999.

[10] Federal Aviation Administration, *Accident and Incident Data*, FAA, 2005.

[11] Chen, J. and Patton, R. J., *Robust model-based fault diagnosis for dynamic systems*, Kluwer Academic Publishers, 1999.

[12] Gertler, J. J., *Fault detection and diagnosis in engineering systems*, Marcel Dekker Inc, New York, 1998.

[13] Patton, R.J., Frank, P.M., Clark, R.N., *Issues of fault diagnosis for dynamic systems*, Springer-Verlag, London, 2000.

[14] Chen, J. and Zhang, H. Y., *Robust detection of faulty actuators via unknown input observers*, International Journal of Systems Science, vol. 22, pp. 1829- 1839, 1991.

[15] Saif, M. and Guan, Y., *A new approach to robust fault detection and identification*, IEEE Trans. on Aerospace and Electronic Systems, vol. 29, No.3, pp. 685-695, 1993.

[16] Van Schrick, D., *Investigations of reliability for instrument fault detection state-estimator schemes*, European Journal of Diagnosis and Safety in Automation, vol. 1, pp. 63-78, 1991.

[17] Patton, R. J., Frank, P. M. and Clark, R. N., *Issues of fault diagnosis for dynamic systems*, Springer, 2000.

[18] Aggoune, W., Boutayeb, M. and Darouach, M., *Observers design for a class of nonlinear systems with time-varying delay*, Proceedings of the 38th Conference on Decision and Control, Phoenix, AZ, pp. 2912- 2913, 1999.

[19] Watanabe, K. and Himmelblau, D. M., *Instrument fault detection in systems with uncertainties*, International Journal of Systems Science, vol. 13, pp. 137-158, 1982.

[20] Seliger, R. and Frank, P. M., *Fault-diagnosis by disturbances decoupled nonlinear observers*, Proceedings of the 30th IEEE Conference on Decision and Control, Brighton, England, pp. 2248-2253, 1991.

[21] Seliger, R. and Frank, P. M., *Robust component fault detection and isolation in nonlinear dynamic systems using nonlinear unknown input observers*, Bibliography 202 Preprints of IFAC/IMACS Symp.: SAFEPROCESS91, Badenbaden, Germany, Vol.1, pp. 313- 318, 1991.

[22] Patton, R., Frank, P. and Clark, R., *Fault Diagnosis In Dynamic Systems: Theory and Application*, Prentice Hall, New York, 1989.

[23] Patton, R. and Chen, J., *Robust fault detection using eigenstructure assignment: a tutorial consideration and some new results*, Proceedings of the 30th IEEE Conference on Decision and Control, Brighton, England, pp. 2242-2247, 1991.

[24] Patton, R. and Chen, J., *A robust parity space approach to fault diagnosis based on optimal eigenstructure assignment*, Proceedings of the IEE International Conference: Control, Edinburgh, England, pp. 1056-1061, 1991.

[25] Slotine, J.-J., Hedrick, E. J. K. and Misawa, E.A., *On sliding observers for nonlinear systems*, Journal of Dynamic Systems, Measurement, and Control, vol. 109, pp. 245-252, 1987.

[26] Yang, H. and Saif, M., *Monitoring and diagnostics of a class of nonlinear systems using a nonlinear unknown input observer*, Proceedings of IEEE Conference on Control Applications, pp. 1006-1011, 1996.

[27] Etkin, B., *Dynamics of Atmospheric Flight*, John Wiley & Son, 1972.

[28] Cook, M.V., *Flight Dynamics Principles*, Arnold, London, 1997.

[29] Stevens, B.L., and Lewis, F.L., *Aircraft Control and Simulation*, John Wiley & Sons, 1992.

[30] Chen, W., *Robust Fault Diagnosis and Compensation in Nonlinear Systems via Sliding Mode and Iterative Learning Observers*, Ph.D Thesis, Simon Fraser University, Nov, 2004

[31] Utkin, V., *Varible structure systems with sliding mode*, IEEE Transactions on Automatic Control, Vol. 22, pp. 212-222, 1977.

[32] Canudas de Wit, C., and Slotine, J.-J. E., *Sliding observers for robot manipulators*, Proceedings of International Federation of Automatic Control, pp. 859-863, 1992.

[33] Helmersson, A. FM(AG08), *Robust Flight Control Design Challenge Problem Formulation and Manual: The Research Civil Aircraft Model (RCAM)*, GARTEUR/TP-088-3, 1996.

[34] Dabroom, A., and Khalil, H.K., *Output Feedback Sampled-Data Control of Nonlinear System Using High-Gain Observers*, IEEE Transactions on Automatic Control, Vol. 46, No.11, pp. 1712-1725, November 2001.

[35] Vidyasagar, M., *Nonlinear Systems Analysis*, Englewood Cliffs, N.J., Prentice Hall, 1978.

[36] Willsky, A. S., *A survey of design methods for failure detection in dynamic systems*, Automatica, vol. 12, pp. 601-611, 1976.

[37] Isermann, R., Supvision, *Fault detection and fault diagnosismethods - an introduction*, Control Engineering Practice, vol. 5, pp. 639-652, 1997.

[38] Gertler, J.J., *Survey of model-based failure detection and isolation in complex plant*, IEEE Control Systems Magazine, vol. 8, pp. 3-11, 1988.

[39] Frank, P.M., *Fault diagnosis in dynamic systems using analytical and knowledge-based redundancy- a survey and some new results*, Automatica, vol. 26, pp. 459-474, 1990.

[40] Edwards, C., Spurgeon, S. K. and Patton, R. J., *Sliding Mode Observers for Fault Detection and Isolation*, Automatica, vol. 36, pp. 541-553, 2000.

[41] Patton, R. J., *Robust model-based fault diagnosis: the state of art*, Proceedings of the IFAC Symposium on Fault Detection, Supervision and Safety for Process(SAFE-PROCESS), Espoo, Finland, pp. 1-24, 1994.

[42] Frank, P.M., *Analytical and qualitative model-based fault diagnosis - a survey and some new results*, European Journal of Control, vol. 2, pp. 6-28, 1996.

[43] Chen, W., Saif, M., *An actuator fault isolation strategy for linear and nonlinear systems*, Proceedings of the American Control Conference, vol. 5, pp. 3321 - 3326, June 2005.

[44] Wang, H. and Daley, S., *Actuator fault diagnosis: an adaptive observer-based technique*, IEEE Transanctions on Automatic Control, vol. 41, No.7, pp. 1073-1078, 1996.

[45] Ahmed-Zaid, F., Ioannou, P., Gousman, K. and Rooney, R., *Accommodation of failures in the F-16 aircraft using adaptive control*, IEEE Control Systems Magazine, vol. 11, No. 1, pp. 73-78, 1991.

[46] Bodson, M., and Groszkiewicz, J.E., *Multivariable adaptive algorithms for reconfigurable flight control*, IEEE Transactions on Control Systems Technology, vol. 5, No. 2, pp. 217-229, 1997.

[47] Boskovic, J.D. and Mehra, R.K., *An adaptive reconfigurable formation flight control design*, Proceedings of the American Control Conference, Denver, Colorado, June 4-6, 2003, pp. 284-289.

[48] Zhang, X., Polycarpou, M. M., and Parisini, T., *A robust detection and isolation scheme for abrupt and incipient faults in nonlinear systems*, IEEE Transactions on Automatic Control, vol. 47, No. 4, pp. 576-593, 2002.

[49] Tao, G., Joshi, S.M., and Ma, X., *Adaptive state feedback and tracking control of systems with actuator failures*, IEEE Transactions on Automatic Control, vol. 46, No. 1, pp. 78-94, 2001.

[50] Tao, G., Chen, S., and Joshi, S.M., *An adaptive actuator failure compensation controller using output feedback* Proceedings of the American Control Conference, Arlington, VA, June 25-27, pp. 3085-3090, 2001.

[51] Tao, G., Chen, S., and Joshi, S.M., *An adaptive control scheme for systems with unknown actuator failures*, Proceedings of the American Control Conference, Arlington, VA, June 25-27, pp. 1115-1120, 2001.

[52] Clark, R. N., *Instrument fault detection*, IEEE Transactions on Aerospace and Electronic Systems, vol. 14, pp. 456-465, 1978.

[53] Walcott, B.L., Corless, M.J. and Zak, S.H., *Comparative study of nonlinear state observation techniques*, International Journal of Control, vol. 45, pp. 2109-2132, 1987.

[54] Helmersson, A., FM(AG08), *Robust Flight Control Design Challenge Problem Formulation and Manual: the Research Civil Aircraft Model (RCAM)*, GARTEUR/TP-088-3, 1996

[55] Pratt, R. J., Roger W., *Flight Control Systems, Practical Issures in Design and Implementation*, IEE Press, 2000.

[56] Chen, W. and Saif, M., *Actuator fault isolation for linear and nonlinear systems*, IEEE Procedings of American Control Conference, 2005.

[57] Clark, R. N., *A simplified instrument fault detection scheme*, IEEE Transactions on Aerospace and Electronic Systems, vol. 14(4), pp. 558-563, 1978.

[58] Frank, P. M., *Failure diagnosis in the dynamic systems via state estimation a Survey in System Fault Diagnostics, Reliability and Related Knowledge-based Approach*, D. Reidel Publishing Company, pp. 35-98, 1987.

[59] Edwards, C. and Spurgeon S., *On the development of discontinuous observers*, International Journal of Control, vol. 59, pp. 1211-1229, 1994.

[60] Chen, W., Jia, G. and Saif, M., *Application of sliding mode observers for actuator fault detection and isolation in linear systems*, Proceedings of IEEE Conference on Control Applications, pp. 1479-1484, Aug., 2005.

[61] Tan, C., and Edwards, C. *An LMI appoach for designing sliding mode observers*, International Journal of Control, Vol. 74, No. 16, pp.1559-1568, 2001

[62] Watanabe, K. and Himmelblau, D. M., *Instrument fault detection in systems with uncertainties*, International Journal of Systems Science, vol. 13(2), pp. 137-158, 1982.

[63] Zhang, X., Polycarpou, M. and Parisini, T., *A robust detection and isolation scheme for abrupt and incipient faults in nonlinear systems*, IEEE Transactions on Automatic Control, vol. 47(4), pp. 576-593, 2002.